

CANCER IMMUNOLOGY

Acquisition of suppressive function by conventional T cells limits antitumor immunity upon T_{reg} depletion

Sarah K. Whiteside^{1*}, Francis M. Grant², Giorgia Alvisi³, James Clarke⁴, Leqi Tang¹, Charlotte J. Imianowski¹, Baojie Zhang¹, Alexander C. Evans¹, Alexander J. Wesolowski¹, Alberto G. Conti¹, Jie Yang¹, Sarah N. Lauder⁵, Mathew Clement⁵, Ian R. Humphreys⁵, James Dooley¹, Oliver Burton¹, Adrian Liston¹, Marco Alloisio^{6,7}, Emanuele Voulaz^{6,7}, Jean Langhorne⁸, Klaus Okkenhaug¹, Enrico Lugli³, Rahul Roychoudhuri^{1*}

Copyright © 2023 The Authors, some rights reserved; exclusive licensee American Association for the Advancement of Science. No claim to original U.S. Government Works

Regulatory T (T_{reg}) cells contribute to immune homeostasis but suppress immune responses to cancer. Strategies to disrupt T_{reg} cell-mediated cancer immunosuppression have been met with limited clinical success, but the underlying mechanisms for treatment failure are poorly understood. By modeling T_{reg} cell-targeted immunotherapy in mice, we find that CD4⁺ Foxp3⁻ conventional T (T_{conv}) cells acquire suppressive function upon depletion of Foxp3⁺ T_{reg} cells, limiting therapeutic efficacy. Foxp3⁻ T_{conv} cells within tumors adopt a T_{reg} cell-like transcriptional profile upon ablation of T_{reg} cells and acquire the ability to suppress T cell activation and proliferation ex vivo. Suppressive activity is enriched among CD4⁺ T_{conv} cells marked by expression of C-C motif receptor 8 (CCR8), which are found in mouse and human tumors. Upon T_{reg} cell depletion, CCR8⁺ T_{conv} cells undergo systemic and intratumoral activation and expansion, and mediate IL-10-dependent suppression of antitumor immunity. Consequently, conditional deletion of IL10 within T cells augments antitumor immunity upon T_{reg} cell depletion in mice, and antibody blockade of IL-10 signaling synergizes with T_{reg} cell depletion to overcome treatment resistance. These findings reveal a secondary layer of immunosuppression by T_{conv} cells released upon therapeutic T_{reg} cell depletion and suggest that broader consideration of suppressive function within the T cell lineage is required for development of effective T_{reg} cell-targeted therapies.

INTRODUCTION

Immune checkpoint blockade therapies targeting the inhibitory receptors PD-1 and CTLA-4 on T_{conv} cells have revolutionized the treatment of advanced cancer (1–5). However, only a minority of patients with a subset of cancers respond to existing therapies (6–8), necessitating development of mechanistically distinct modes of immunotherapy. Regulatory T (T_{reg}) cells play a critical role in suppressing antitumor immunity (9–14). High relative ratios of T_{reg} cells to CD4⁺ or CD8⁺ conventional T (T_{conv}) cells within tumors are associated with poor prognoses in patients with a variety of cancers, including ovarian cancer (15, 16), breast cancer (17), non-small cell lung carcinoma (18), hepatocellular carcinoma (19), renal cell carcinoma (20), pancreatic cancer (21), gastric cancer (22), cervical cancer (23), intrahepatic cholangiocarcinoma (24), and colorectal carcinoma (25). Foxp3⁺ T_{reg} cells also contribute to immunotherapy resistance, including to immune checkpoint inhibitor therapy (18, 26–28). There is intense medical interest in therapeutically depleting T_{reg} cells or modulating their immunosuppressive function in cancer patients.

Despite abundant experimental evidence of the immunosuppressive role of T_{reg} cells in cancer, T_{reg} cell-targeted therapies have

had limited success in the clinic. Agents developed for depletion of T_{reg} cells in humans have included daclizumab (Zenapax), a monoclonal antibody against CD25, which is expressed highly on the surface of most T_{reg} cells, denikeukin ditox (Ontak), an interleukin-2 (IL-2):diphtheria toxin (DTx) fusion protein that targets T_{reg} cells through their ability to bind IL-2, and mogamulizumab, a depleting monoclonal antibody against CCR4, which is expressed by high frequencies of tumor-infiltrating T_{reg} cells (29). Daclizumab therapy failed to enhance the efficacy of a dendritic cell vaccine in patients with metastatic melanoma (30) and only modestly increased immune response parameters in patients with glioblastoma (31) and breast cancer (32), whereas denikeukin ditox treatment failed to induce clinical responses in patients with metastatic melanoma (33). Mogamulizumab therapy lacked antitumor efficacy in patients with advanced cancer (34), likely attributable to concomitant depletion of activated CD4⁺ and CD8⁺ T_{conv} cells expressing CCR4 (35). Lack of robust clinical efficacy in many cases indicates a need to discern the basis for treatment failure of T_{reg} cell-targeted therapies.

Here, we sought to better understand mechanisms of treatment failure of T_{reg} cell-targeting cancer immunotherapies. We systematically evaluated the consequence of experimental T_{reg} cell ablation on T_{conv} cells within tumors. Whereas CD4⁺ and CD8⁺ T_{conv} cells were markedly transcriptionally distinct from T_{reg} cells under steady-state conditions, T_{reg} cell ablation caused T_{conv} cells to adopt a T_{reg} cell-like transcriptional profile, up-regulating expression of molecules associated with T_{reg} cell-suppressive function. Consistent with acquisition of a T_{reg} cell-like transcriptional profile, Foxp3⁻ T_{conv} cells from T_{reg} cell-depleted animals acquired the ability to suppress T_{conv} cell activation and proliferation in vitro, attributable to a subset of T_{conv} cells marked by expression of CCR8. This subset of suppressive T_{conv} cells was enriched in both murine and human tumors, and its

¹Department of Pathology, University of Cambridge, Tennis Court Road, Cambridge, CB2 1QP, UK. ²Immunology Programme, Babraham Institute, Babraham Research Campus, Cambridge, Cambridgeshire CB22 3AT, UK. ³Laboratory of Translational Immunology, IRCCS Humanitas Research Hospital, Via Manzoni 56, 20089 Rozzano, Milan, Italy. ⁴La Jolla Institute for Allergy and Immunology, La Jolla, CA, USA. ⁵Division of Infection and Immunity/System Immunology Research Institute, Cardiff University, Cardiff CF14 4XN, UK. ⁶Department of Biomedical Sciences, Humanitas University, Via Rita Levi Montalcini 4, 20072 Pieve Emanuele, Milan, Italy. ⁷Division of Thoracic Surgery, IRCCS Humanitas Research Hospital, Via Manzoni 56, 20089 Rozzano, Milan, Italy. ⁸Francis Crick Institute, 1 Midland Road, London NW1 1AT, UK.

*Corresponding author. Email: sw925@cam.ac.uk (S.K.W.); rr257@cam.ac.uk (R.R.)

suppressive function was dependent on IL-10. Consequently, conditional deletion of *Il10* specifically within T cells and blockade of IL-10 receptor (IL-10R) signaling during T_{reg} cell-depleting immunotherapy reduced treatment resistance and resulted in enhanced tumor clearance. These findings indicate that compensatory suppression by T_{conv} cells limits efficacy of T_{reg} cell-targeted therapeutic depletion and suggest that broader consideration of suppressive activity within the T cell lineage is required for development of more effective therapies.

RESULTS

T_{reg} cell depletion causes T_{conv} cells to adopt a T_{reg} cell-like transcriptional profile

T_{reg} cell depletion has had limited success in cancer patients with advanced disease. To better understand the mechanisms underlying treatment failure in the context of therapeutic T_{reg} cell ablation, we used *Foxp3*^{EGFP-DTR} mice, which express human diphtheria toxin receptor (DTR) and enhanced green fluorescent protein (EGFP) under the transcriptional control of the endogenous *Foxp3* gene. Administration of DTx to *Foxp3*^{EGFP-DTR} mice enables selective depletion of Foxp3⁺ T_{reg} cells (36). We subcutaneously implanted syngeneic B16-F10 melanoma cells into *Foxp3*^{EGFP-DTR} mice and ablated T_{reg} cells through administration of DTx. Early T_{reg} cell ablation (before tumors were palpable) resulted in incomplete rejection of primary tumors, whereas T_{reg} cell depletion in mice with established tumors had little discernible effect on tumor growth (Fig. 1A), despite near-complete ablation of Foxp3-expressing T_{reg} cells within the systemic and intratumoral compartments of DTx-treated mice (Fig. 1B).

To understand mechanisms of treatment resistance, we examined the consequence of T_{reg} cell depletion on the transcriptional profiles of CD4⁺ and CD8⁺ T_{conv} cells within tumors. Although intratumoral *Foxp3*^{EGFP-} CD4⁺ and CD8⁺ T_{conv} cells were markedly transcriptionally distinct from *Foxp3*^{EGFP+} T_{reg} cells under steady-state conditions, T_{reg} cell depletion caused *Foxp3*^{EGFP-} T_{conv} cells to adopt a T_{reg} cell-like transcriptional profile. We noted that a large proportion of genes specifically enriched within tumor-associated T_{reg} cells compared with CD4⁺ T_{conv} cells [$|fold\ change\ (FC)| > 4, q < 0.05$] under steady-state conditions were induced at high levels within CD4⁺ or CD8⁺ T_{conv} cells upon T_{reg} cell ablation (Fig. 1, C and D, and data file S1). Clusters A and B comprised intratumoral T_{reg} cell-associated genes up-regulated in both CD4⁺ and CD8⁺ T_{conv} cells upon T_{reg} cell depletion; cluster C contained intratumoral T_{reg} cell-associated genes whose expression was up-regulated exclusively in CD8⁺ T_{conv} cells; cluster D included intratumoral T_{reg} cell-associated genes whose expression was up-regulated exclusively in CD4⁺ T_{conv} cells; cluster E comprised a limited set of T_{reg} cell-specific transcripts that were not expressed at high relative levels in CD4⁺ or CD8⁺ T_{conv} cells even upon T_{reg} depletion, including *Foxp3*, *Lrrc32*, *Ikzf2*, and *Ctla4*. Similarly, a substantial fraction of transcripts highly expressed within intratumoral T_{conv} cells compared with T_{reg} cells were down-regulated within T_{conv} cells upon T_{reg} cell ablation (fig. S1 and data file S2). Consistent with these observations, hierarchical clustering analysis of Pearson distances between global transcriptional profiles of samples revealed that intratumoral CD4⁺ and CD8⁺ T_{conv} cells from T_{reg} cell-depleted animals clustered more strongly with T_{reg} cells than T_{conv} cells from T_{reg} cell-sufficient animals (Fig. 1E). Moreover, differences in gene expression between CD4⁺ T_{conv} cells in the absence versus presence of T_{reg} cells were positively correlated with differences

in gene expression between intratumoral T_{reg} cells and CD4⁺ T_{conv} cells from T_{reg} cell-sufficient animals (Fig. 1F). Collectively, these results show that intratumoral T_{conv} cells adopt a T_{reg} cell-like transcriptional profile upon experimental ablation of T_{reg} cells in vivo.

Ablation of T_{reg} cells promotes the induction of T_{conv} cell-mediated suppression

T_{reg} cells suppress the proliferation of naïve T_{conv} cells when cocultured in vitro (37–39). Given their acquisition of a T_{reg} cell-like transcriptional profile, we asked whether T_{conv} cells develop suppressive function upon depletion of T_{reg} cells. To test this, we purified *Foxp3*^{EGFP-} CD4⁺ T_{conv} cells or *Foxp3*^{EGFP+} CD4⁺ T_{reg} cells by fluorescence-activated cell sorting (FACS) from B16-F10 tumor-bearing *Foxp3*^{EGFP-DTR} mice and incubated them with congenically distinct naïve CD4⁺ T_{conv} cells in vitro (Fig. 2A and fig. S2). Strikingly, CD4⁺ T_{conv} cells from the tumors of mice whose T_{reg} cells had been ablated by administration of DTx profoundly suppressed the proliferation of naïve CD4⁺ responder T (T_{resp}) cells compared with CD4⁺ T_{conv} cells from tumors of animals with intact T_{reg} cell populations (Fig. 2, B and C). The level of suppression was only marginally less than the level of suppressive activity of a similar number of intratumoral Foxp3⁺ T_{reg} cells. We observed lower levels of suppressive activity among splenic T_{conv} cells (fig. S3, A and B), suggesting that suppressive function was enriched in the tumor. In addition to suppressing T cell proliferation, T_{conv} cells from tumors of T_{reg} cell-depleted animals suppressed stimulation-driven induction of the activation marker CD44 on responder T cells in contrast to T_{conv} cells from tumors of non-T_{reg} cell-depleted animals (Fig. 2, D and E). T_{conv} cells from T_{reg} cell-depleted animals expressed similar levels of the coinhibitory molecules TIGIT, TIM-3, and GITR to intratumoral T_{reg} cells (Fig. 2, F and G). They also expressed higher levels of CTLA-4 and ICOS compared with CD4⁺ T_{conv} cells from tumors with intact T_{reg} cell populations. Acquisition of suppressive function by T_{conv} cells was not an artifact of DTx treatment, because administration of DTx to *Foxp3*^{EGFP-DTR} and control *Foxp3*^{EGFP} mice resulted in induction of potent suppressive activity only among CD4⁺ T_{conv} cells from *Foxp3*^{EGFP-DTR} animals, whose T_{reg} cells are sensitive to DTx treatment (fig. S3, C and D). Thus, upon T_{reg} cell depletion, CD4⁺ T_{conv} cells within tumors acquire transcriptional and functional characteristics of T_{reg} cells.

T_{reg} cell depletion results in activation and expansion of CCR8⁺ T_{conv} cells

To understand whether changes in the transcriptional and functional properties of bulk populations of T_{conv} cells in the absence of T_{reg} cells were driven by specific subpopulations, we performed single-cell RNA sequencing (scRNA-Seq) of bulk T cell populations sorted by FACS from B16-F10 melanoma tumors of DTx- and phosphate-buffered saline (PBS)-treated *Foxp3*^{EGFP-DTR} animals at day 16 after tumor implantation. Single-cell gene expression data were clustered using Seurat, and global transcriptional differences between cells were visualized in two-dimensional space using Uniform Manifold Approximation and Projection (UMAP). k-means clustering revealed the presence of eight transcriptionally distinct clusters of cells (Fig. 3A). Clusters 2 and 3 were enriched in control samples, whereas clusters 0, 1, 5, and 7 were enriched among T cells from tumors of T_{reg} cell-depleted animals (Fig. 3, B and C). Enrichment analysis was used to determine which cell cluster was most responsible for the induction of T_{reg} cell-like gene expression within bulk RNA-Seq

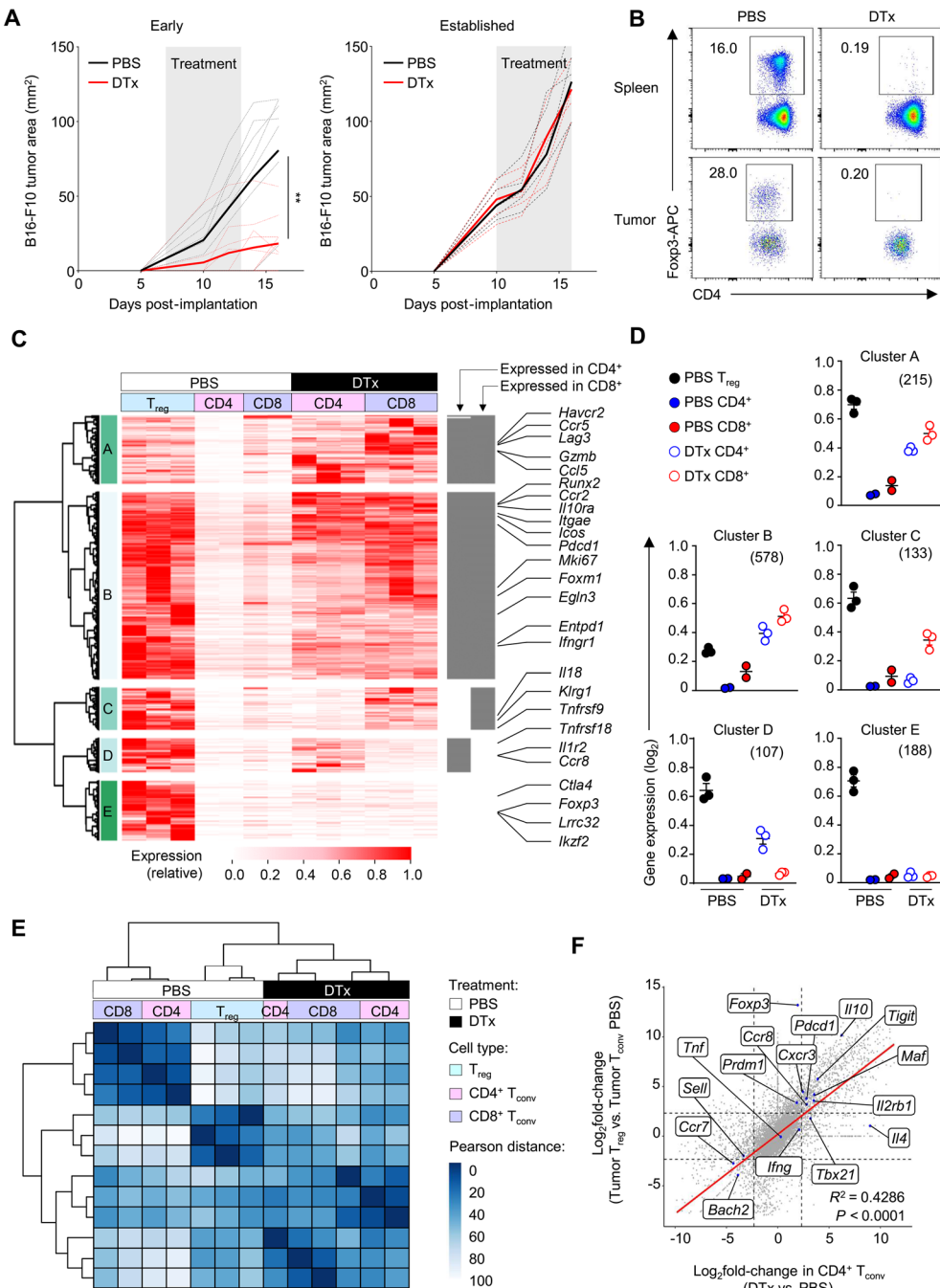


Fig. 1. T_{reg} cell ablation causes T_{conv} cells to acquire transcriptional features of T_{reg} cells. (A) Tumor growth of B16-F10 tumors subcutaneously implanted into *Foxp3*^{EGFP-DTR} mice. Gray shading indicates time period over which PBS or DTx was administered (days 7 to 13 after implantation, early disease; days 10 to 16 after implantation, established). Dashed lines indicate individual mice. Solid line indicates average tumor area over time. Data are representative of three individually repeated experiments. $n > 5$. ** $P < 0.01$, two-tailed Mann-Whitney U test. (B) Representative frequency of Foxp3⁺ T_{reg} cells among total CD4⁺ T cells within spleens (top) or tumors (bottom) of *Foxp3*^{EGFP-DTR} mice with established tumors, administered with PBS or DTx. (C) Heatmap showing the relative expression of intratumoral T_{reg} cell-expressed transcripts (genes up-regulated in intratumoral T_{reg} cells compared with CD4⁺ T_{conv} cells; $p < 0.05$; FC > 4) in the indicated T cell populations isolated on day 18 after implantation of B16-F10 tumors in *Foxp3*^{EGFP-DTR} animals and administration of PBS or DTx. Colors indicate expression normalized to row maxima. X-axis hierarchical clustering of intratumoral T_{reg} cell-expressed transcripts identifies five clusters of genes with distinct expression patterns. Gray bars to the right of the heatmap indicate expression greater than a third of the expression of given transcripts in intratumoral T_{reg} cells. (D) Average expression of genes within the five clusters identified in each T cell subset. (E) Heatmap showing pairwise Pearson distances between the global gene expression profiles of the indicated T cell subsets from B16-F10 tumor-bearing *Foxp3*^{EGFP-DTR} animals administered PBS or DTx. (F) Scatterplot comparing the global differences in gene expression between intratumoral T_{reg} cells and T_{conv} cells with transcriptional differences between CD4⁺ T_{conv} cells isolated from DTx versus PBS-treated animals. A highly significant correlation is observed, indicating transcriptional convergence of intratumoral T_{reg} cells with T_{conv} cells in the absence of T_{reg} cells. Data are from two to four biological replicates isolated on independent days (C to F).

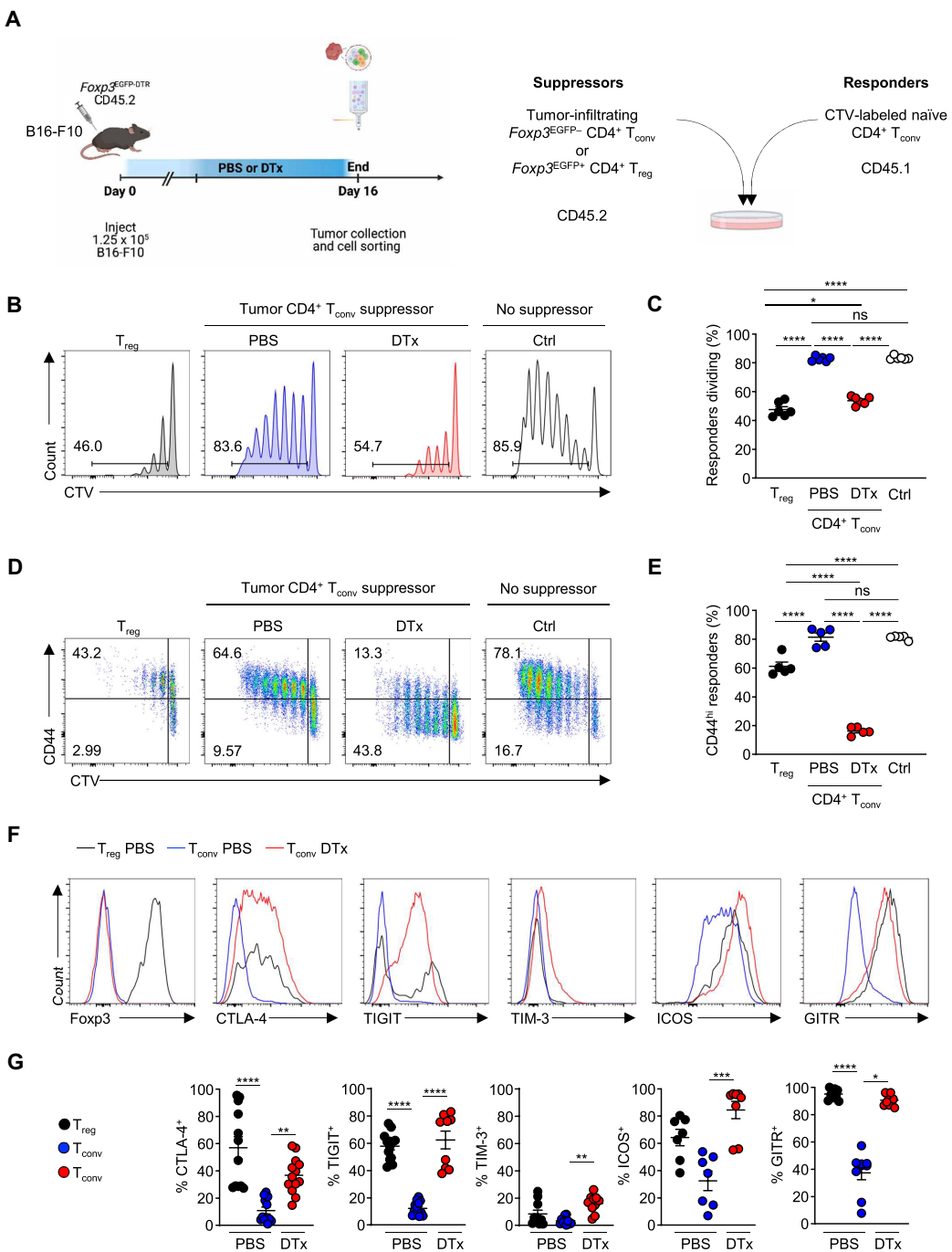


Fig. 2. T_{reg} cell depletion causes CD4⁺ T_{conv} cells to acquire suppressive function. (A) Experimental schema. B16-F10 cells were subcutaneously implanted into *Foxp3^{EGFP-DTR}* CD45.2⁺ mice and administered with PBS or DTx on days 7, 9, 11, and 13. Cells were harvested from tumors 16 days after implantation and used in suppression assays. (B and C) In vitro suppression assay. Proliferation of naïve CD45.1⁺ CD4⁺ T_{resp} cells cultured for 4 days at a 4:1 ratio with indicated suppressor cell populations [*Foxp3^{EGFP-}* T_{conv} cells from tumors of T_{reg} cell–replete (PBS) or T_{reg}–depleted (DTx) mice or GFP⁺ T_{reg} cells from tumors of T_{reg} cell–replete mice]. Representative histograms and replicate measurements of proliferation dye dilution 4 days after stimulation, gated on CD45.1⁺ T_{resp} cells, are shown. T_{resp} cell proliferation in the absence of a suppressor cell population was used as a control. Suppressor cells were cocultured with T_{resp} cells at a ratio of 1:4, with 2.5 × 10⁴ suppressor CD4⁺ T_{reg} or T_{conv} cells cocultured with 1 × 10⁵ T_{resp} cells in the presence of 5.0 × 10⁴ APCs. Data are representative of more than four independently repeated experiments, n > 5 per group; ordinary one-way ANOVA, Tukey's multiple comparisons. (D and E) Representative histograms and replicate measurements of CD44 expression by CD45.1⁺ T_{resp} cells incubated with indicated suppressor cell populations. (F and G) Representative flow cytometry and replicate measurements of the expression of the indicated proteins by intratumoral T_{reg} cells and CD4⁺ T_{conv} cells isolated at day 16 after implantation of B16-F10 tumors in *Foxp3^{EGFP-DTR}* mice treated with PBS or DTx. Data are representative of more than three independently repeated experiments, n > 7 per group. ****P < 0.0001; ns, not significant; one-way ANOVA Kruskal-Wallis, Dunn's multiple comparisons test. Error bars show SEM.

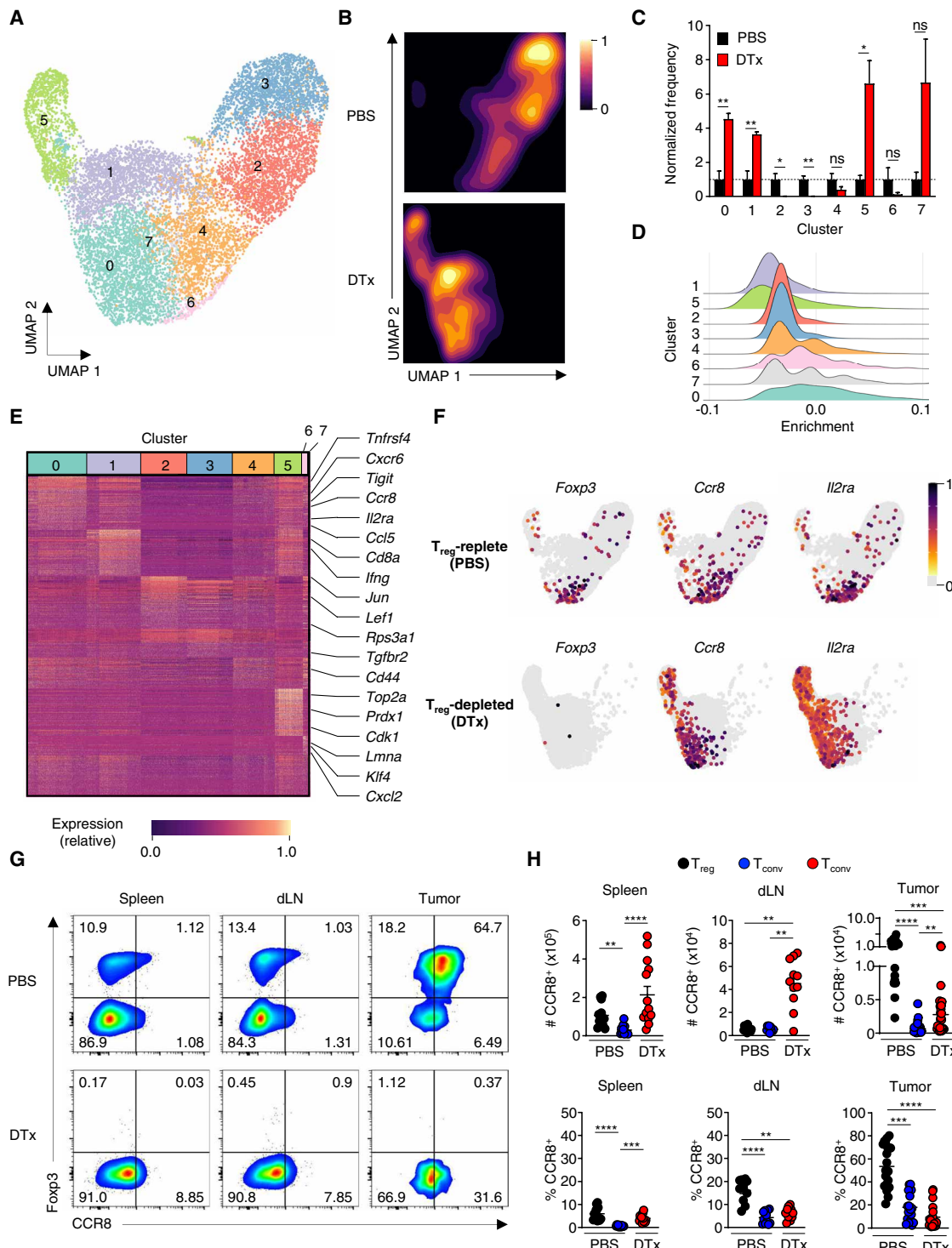


Fig. 3. T_{reg} cell depletion promotes the expansion of tumor-infiltrating $CCR8^+$ T_{conv} cells. (A) UMAP of scRNA-Seq analysis of $TCR\beta^+$ cells isolated at day 16 after implantation of B16-F10 tumors in $Foxp3^{EGFP-DTR}$ mice treated with PBS or DTx on days 7, 9, 11, and 13. (B) Density plots showing change in distribution of cells within tumors of T_{reg} cell-replete (PBS) and T_{reg} cell-depleted (DTx) animals. (C) Relative frequency of cells within each cluster normalized to their average ratio among PBS animals. $n = 3$ biological replicates per group. (D) Average enrichment of expression of the genes in cluster D from Fig. 1C across scRNA-Seq clusters ($n = 3$, unpaired two-tailed Student's t test, $*P < 0.05$, $**P < 0.01$). (E) Heatmap showing the expression of differentially up-regulated genes in each cluster identified. (F) UMAP plots showing expression of indicated genes within T cells of tumors from tumor-bearing PBS- or DTx-treated $Foxp3^{EGFP-DTR}$ animals. (G) Representative flow cytometry and (H) replicate measurements of total counts (top) and the frequency (bottom) of $CCR8^+$ cells among $CD4^+$ T_{conv} cells from spleens, dLN, and tumors of B16-F10 tumor-bearing $Foxp3^{EGFP-DTR}$ mice treated with PBS or DTx. Data are representative of three independently repeated experiments (G and H). Numbers in gates show percentages. $n > 10$, one-way ANOVA Kruskal-Wallis, Dunn's multiple comparisons test. $**P < 0.01$, $***P < 0.001$, $****P < 0.0001$. Error bars show SEM.

profiles of T_{conv} cells from T_{reg} cell-depleted animals. This revealed that cluster 0 (present at a ~3:1 ratio in the DTx treatment condition) was most enriched in genes specifically up-regulated by CD4⁺ T_{conv} cells upon DTx treatment (Fig. 3D). To define surface markers that would enable isolation of cells of cluster 0, we performed an analysis of uniquely enriched up-regulated transcripts within each cluster. This analysis revealed that cluster 0 cells express transcripts associated with T cell activation but that are also highly expressed by T_{reg} cells, including *Il2ra*, *Tigit*, and *Tnfrsf4* (Fig. 3E and data file S3). Strikingly, *Ccr8* mRNA expression was also up-regulated in cluster 0 cells upon depletion of T_{reg} cells, which was notable because we and others have shown that the encoded protein chemokine (C-C motif) receptor 8 (CCR8) marks highly suppressive T_{reg} cells under steady-state conditions within both murine and human tumors (40–44). A focused analysis of the CD4⁺ T cells in cluster 0 revealed a subpopulation of cells (subcluster 5) enriched in expression of transcripts encoding proteins associated with T helper 2 (T_H2) differentiation, including *Ccr8*, *Gata3*, *Maf*, and *Il10*, and suppressive/coinhibitory function, including *Pdcld1*, *Tigit*, *Il10*, and *Lag3* (fig. S4 and data file S4). Accordingly, an analysis of the distribution of cells expressing *Ccr8*, *Il2ra*, *Tigit*, and *Tnfrsf4* revealed that whereas in T_{reg} cell-replete animals these markers are largely expressed by intratumoral *Foxp3*^{EGFP+} T_{reg} cells, they were up-regulated by a subset of *Foxp3*^{EGFP-} CD4⁺ T_{conv} cells upon T_{reg} cell depletion (Fig. 3F and fig. S5).

We therefore analyzed the expression of CCR8 on the surface of T_{reg} and T_{conv} cells in tumors and lymphatics of *Foxp3*^{EGFP-DTR} animals treated with PBS or DTx (Fig. 3, G and H). We found that T_{reg} cell depletion increased the absolute number of CCR8⁺ T_{conv} cells within all tissues analyzed, including tumors, draining lymph nodes (dLN), and spleen, whereas the relative frequency of CCR8⁺ cells among total CD4⁺ *Foxp3*^{EGFP-} T_{conv} cells was increased within the spleens of T_{reg} cell-depleted animals, but not within dLN and tumors because of the absolute expansion of other CD4⁺ *Foxp3*^{EGFP-} T_{conv} cell subsets in these tissues upon T_{reg} cell depletion.

CCR8 expression marks highly suppressive T_{conv} cells within tumors

To better understand the identity of CCR8⁺ T_{conv} cells, we purified CCR8⁺ and CCR8⁻ CD4⁺ T_{conv} cells by FACS from B16-F10 tumors of DTx-treated *Foxp3*^{EGFP-DTR} mice and subjected them to bulk RNA-Seq. CCR8⁺ T_{conv} cells were enriched in transcripts encoding molecules associated with both T cell activation such as *Tnfrsf9* (encoding 4-1BB) and T_{reg} cell-suppressive function, including *Il2ra*, *Areg*, and *Il10* (Fig. 4A and data file S5). CCR8⁺ T_{conv} cells were not enriched in transcripts associated with suppressive type 1 regulatory T cells (Tr1) such as *Eomes*, *Gzmk*, *Itga2* (encoding CD49b), *Ccr5*, or *Cd226*, suggesting that they are distinct from Tr1 cells. Gene set enrichment analysis (GSEA) of global gene expression differences between CCR8⁺ and CCR8⁻ T_{conv} cells revealed a negative enrichment of genes up-regulated in *Foxp3*⁻ T_{conv} cells versus *Foxp3*⁺ T_{reg} cells among CCR8⁺ T_{conv} cells compared with CCR8⁻ T_{conv} cells (Fig. 4B). Consistently, we observed that global differences in gene expression between CCR8⁺ and CCR8⁻ T_{conv} cells were positively correlated with global differences in gene expression between intratumoral T_{reg} and T_{conv} cells (Fig. 4C), further suggesting that CCR8 expression marks *Foxp3*⁻ T_{conv} cells enriched with a T_{reg} cell-like transcriptional profile.

We compared the phenotype of CCR8⁻ and CCR8⁺ CD4⁺ T_{conv} cells from the tumors of mice whose T_{reg} cells had been depleted by

DTx with that of T_{reg} cells. Like T_{reg} cells, we found that CCR8⁺ CD4⁺ T_{conv} cells expressed high levels of CD25, OX40, GITR, TIGIT, and LAG-3 compared with CCR8⁻ CD4⁺ T_{conv} cells (Fig. 4, D and E). CCR8⁺ T_{conv} cells also expressed increased levels of the transcription factor GATA3, suggesting that they have a T_H2-like differentiation state. To test whether CCR8⁺ cells that accumulate within intratumoral T_{conv} cell populations after T_{reg} cell ablation have increased suppressive activity, we separately sorted CCR8⁺ and CCR8⁻ *Foxp3*^{EGFP-} T_{conv} cells from the tumors of DTx-treated *Foxp3*^{EGFP-DTR} mice and assessed their ability to suppress naïve T_{conv} cell proliferation in vitro. Notably, suppressive function was enriched within the CCR8⁺ T_{conv} cell fraction, which was more capable of restricting proliferation of responder cells compared with the CCR8⁻ T_{conv} cell fraction (Fig. 4, F and G). Together, these results suggest that CCR8 expression marks a subset of highly activated and suppressive T_{conv} cells, which accumulate systemically and within tumors upon T_{reg} cell depletion.

CD4⁺ FOXP3⁻ CCR8⁺ T_{conv} cells are found within tumors of NSCLC patients

To determine whether CCR8⁺ FOXP3⁻ T_{conv} cells are enriched in human tumors, we analyzed CD4⁺ T cells from 48 patients with non–small cell lung carcinoma (NSCLC) by flow cytometry (fig. S6). Similar to our observations in mouse, CCR8⁺ FOXP3⁻ T_{conv} cells expressed high levels of CD25 and were enriched in tumor tissue compared with healthy adjacent tissue and blood from the same patients (Fig. 5, A and B). The frequency of CCR8⁺ CD25⁺ FOXP3⁻ T_{conv} cells was inversely correlated with the frequency of cytotoxic CD8⁺ T cells within tumors (Fig. 5C). They also coexpressed the inhibitory receptors PD-1, TIGIT, and TIM-3 (Fig. 5, D and E). CD4⁺ FOXP3⁻ CCR8⁺ T cells displayed increased expression of the tissue residency marker CXCR6 and costimulatory receptor CD27 compared with CCR8⁻ cells, and their phenotype was largely overlapping with that of FOXP3⁺ T_{reg} cells (Fig. 5, E and F). CD4⁺ FOXP3⁻ CCR8⁺ T cells lacked expression of EOMES and granzyme K, providing further evidence that this cell type is distinct from Tr1 cells (Fig. 5E). The presence of CCR8⁺ FOXP3⁻ T_{conv} cells in human tumors under steady-state conditions and without T_{reg} cell depletion is consistent with our observations within murine tumors (Fig. 3H), which contain a population of CCR8⁺ CD4⁺ T_{conv} cells under basal conditions that undergo numeric expansion upon T_{reg} cell ablation.

IL-10-dependent immunosuppression by T_{conv} cells limits efficacy of T_{reg} cell depletion

We sought to understand how intratumoral CD4⁺ T_{conv} cells exert their suppressive function. Informed by the results of our transcriptional analyses, we screened for the involvement of candidate suppressive mechanisms by which T_{conv} cells from T_{reg} cell-depleted animals suppress T cell activation and proliferation in vitro. We tested whether blocking antibodies directed against CD25, CTLA-4, IL-10R, and CCR8; neutralizing antibodies specific for transforming growth factor-β (TGF-β); or pharmacological inhibition of steroid biosynthesis preferentially produced by T_H2 cells using aminoglutethimide (AG) (45) is able to reverse the suppressive activity of intratumoral T_{conv} cells from T_{reg} cell-depleted animals. Although the proliferation of naïve CD4⁺ T cells was suppressed by *Foxp3*⁻ T_{conv} cells, differences induced by the presence of suppressive *Foxp3*⁻ T_{conv} cells were abolished upon treatment of cells with anti-IL-10R blocking antibodies (Fig. 6, A and B).

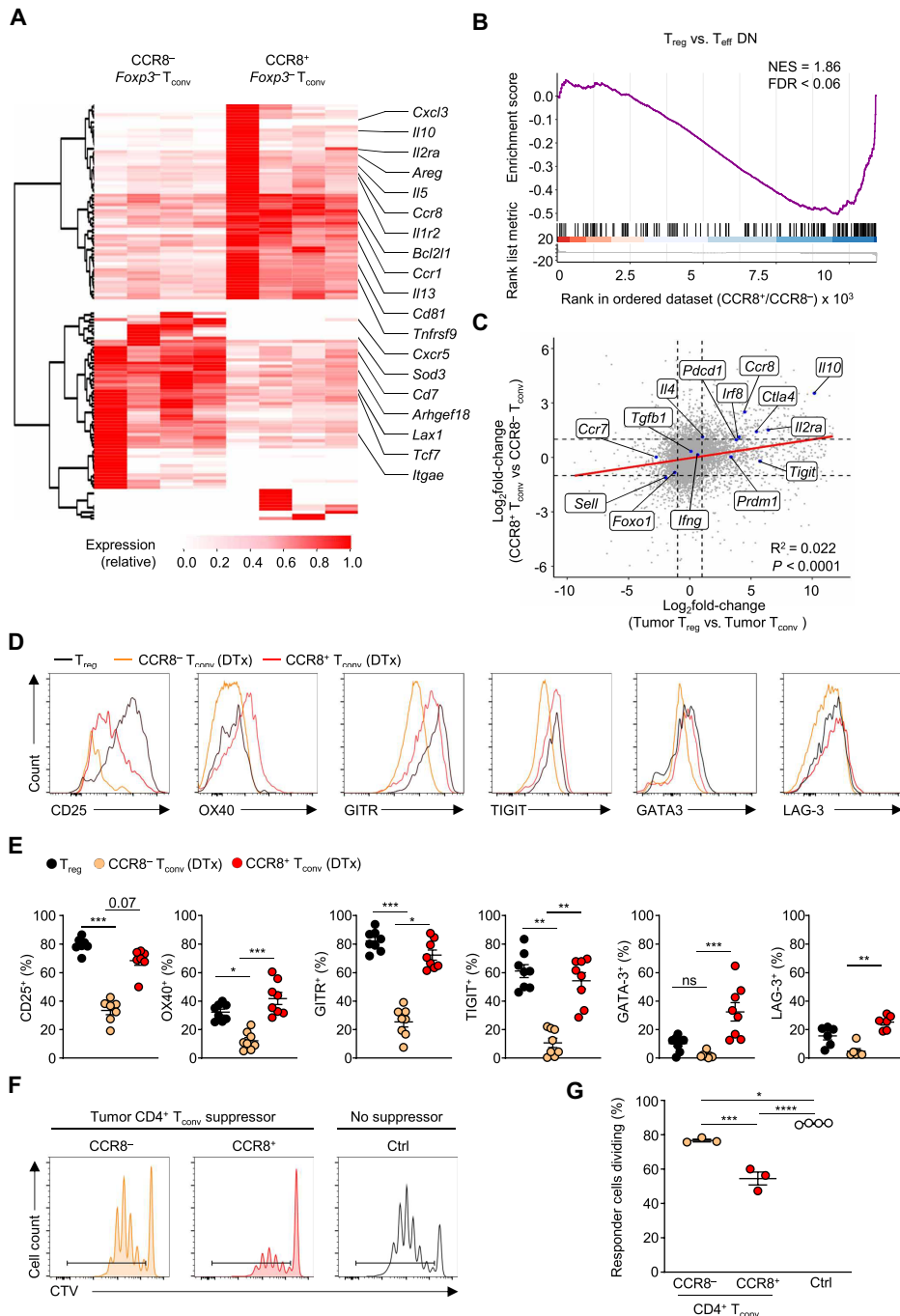


Fig. 4. CCR8 marks highly suppressive T_{conv} cells. (A) Heatmap showing the relative expression of differentially expressed genes between intratumoral CCR8⁺ and CCR8⁻ CD4⁺ T_{conv} cells ($q < 0.05$; $|FC| > 3$) isolated from tumors of B16-F10-bearing *Foxp3*^{EGFP-DTR} animals treated with DTx at days 7, 9, 11, and 13 after tumor implantation. Data are from four biological replicates isolated on the same day. (B) GSEA demonstrating a negative enrichment of genes up-regulated in *Foxp3⁻T_{conv}* cells versus *Foxp3⁺T_{reg}* cells among CCR8⁺ T_{conv} cells compared with CCR8⁻ T_{conv} cells isolated from tumors of DTx-treated *Foxp3*^{EGFP-DTR} mice. (C) Scatterplot comparing global changes in gene expression between intratumoral T_{reg} and T_{conv} cells with transcriptional differences between CCR8⁺ and CCR8⁻ CD4⁺ T_{conv} cells. (D) Representative flow cytometry and (E) replicate measurements of the expression of the indicated proteins by intratumoral T_{reg} cells, and CCR8⁺ and CCR8⁻ CD4⁺ T_{conv} cells from tumors of B16-F10 tumor-bearing *Foxp3*^{EGFP-DTR} mice treated with PBS or DTx. Data are representative of three independently repeated experiments. $n > 4$, one-way ANOVA Kruskal-Wallis, Dunn's multiple comparisons test. * $P < 0.05$, ** $P < 0.01$, *** $P < 0.001$, **** $P < 0.0001$. (F) Representative histograms and (G) replicate measurements of proliferation dye dilution by T_{resp} cells (naïve CD45.1⁺ CD4⁺ T_{conv} cells) incubated with intratumoral CD45.2⁺ TCR β^+ CD4⁺ GFP⁻ CCR8⁻ or CD45.2⁺ TCR β^+ CD4⁺ GFP⁻ CCR8⁺ T_{conv} cells isolated at day 16 after implantation of B16-F10 tumors in *Foxp3*^{EGFP-DTR} mice administered with DTx. Suppressor cells were incubated with responders at a ratio of 1:8, with 1.25×10^4 suppressor CD4⁺ T_{conv} cells cocultured with 1×10^5 T_{resp} cells in the presence of 5×10^4 APCs. Cell proliferation of T_{resp} cells was analyzed after 4 days. Data are representative of two independently repeated experiments. $n > 3$, ordinary one-way ANOVA, Tukey's multiple comparisons. * $P < 0.05$; *** $P < 0.001$, **** $P < 0.0001$. Error bars show SEM.

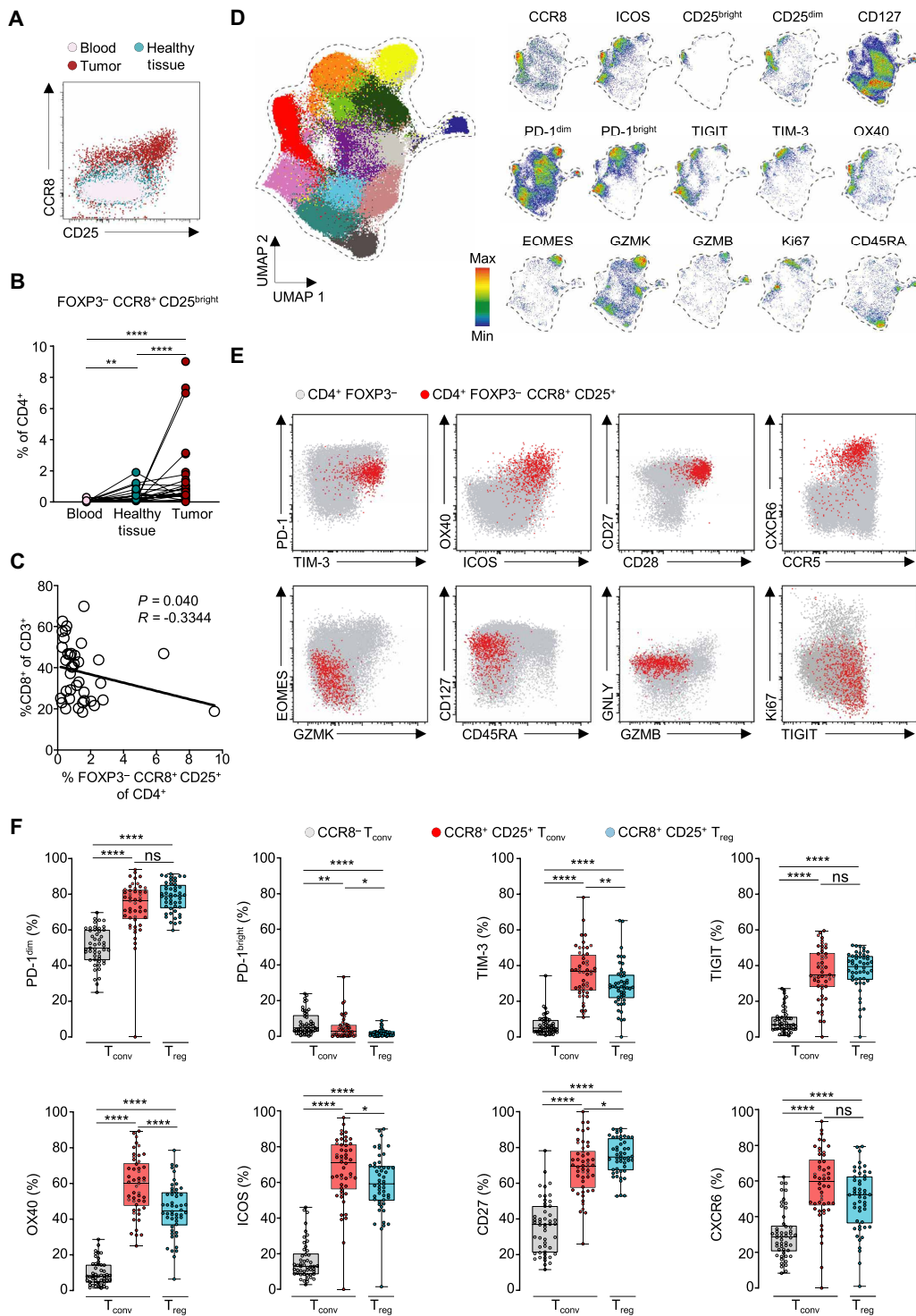


Fig. 5. CCR8⁺ T_{conv} cells expressing high levels of CD25 are found within the tumors of patients with NSCLC. (A) CCR8 and CD25 expression among FOXP3⁻ CD4⁺ T cells within representative samples from patients with NSCLC ($n = 48$). (B) Frequency of FOXP3⁻ CCR8⁺ CD25^{bright} cells among CD4⁺ T cells from the indicated patients' samples. Lines indicate paired samples. (C) Correlation of the frequency of CD8⁺ T cells (of CD3⁺ T cells) with FOXP3⁻ CCR8⁺ CD25^{bright} cells (of CD4⁺ T cells) in tumors from patient samples. (D) UMAP analysis of concatenated CD4⁺ FOXP3⁻ T_{conv} cells (left). Colors depict cell clusters identified by PhenoGraph ($k = 500$). Separate UMAP plots of relative marker expression by concatenated CD4⁺ T cells from tumors (right). (E) Representative frequency and (F) replicate measurements of indicated markers from patient samples. Box plots show median and interquartile range (IQR). Bars indicate SD. Dots depict values of a single tumor sample. ** $P < 0.01$, *** $P < 0.001$, **** $P < 0.0001$; two-tailed Mann-Whitney U test.

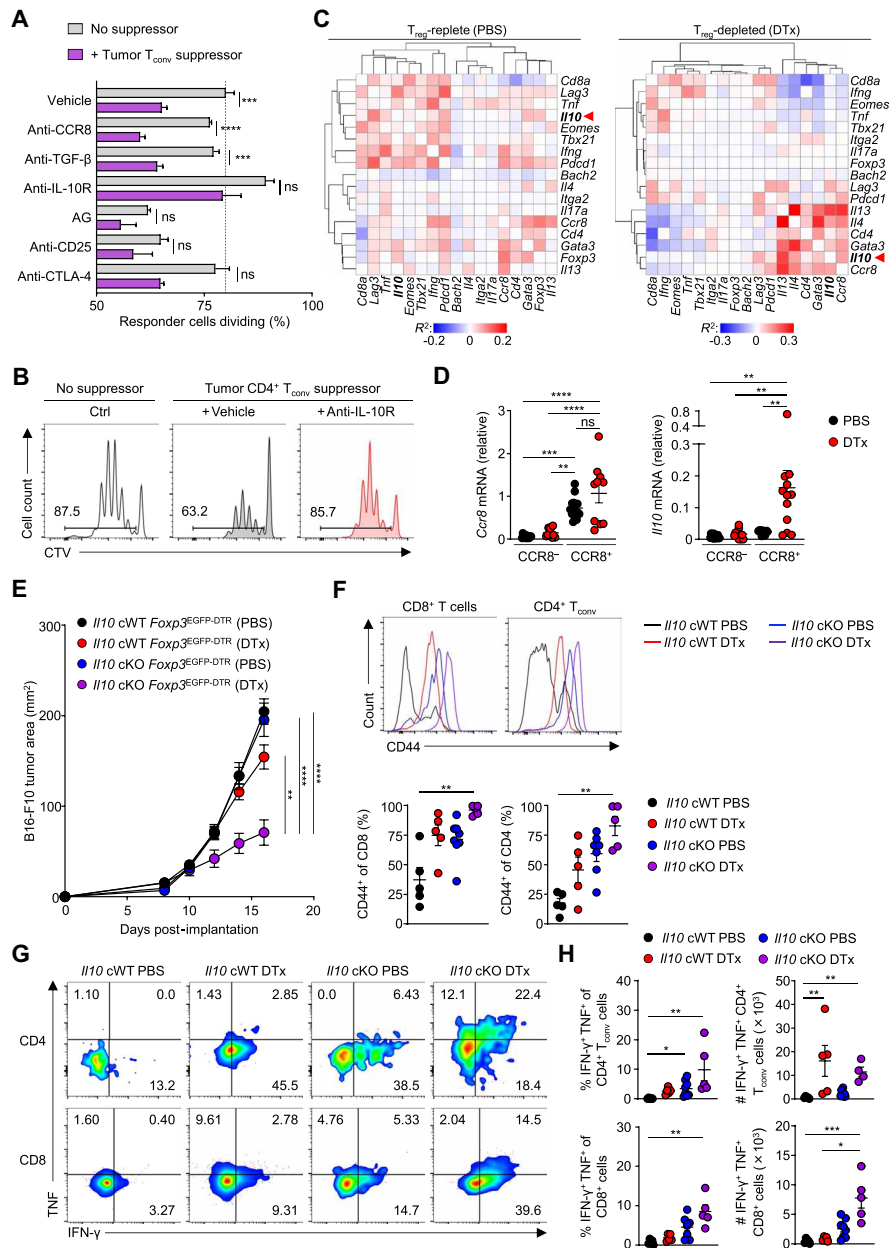


Fig. 6. IL-10 production by $CD4^+ T_{\text{conv}}$ cells limits antitumor immunity upon T_{reg} cell depletion. (A) Screen to identify mechanisms of immune suppression by $CD4^+ T_{\text{conv}}$ cells from tumors of T_{reg} cell-depleted animals. Proliferation of CTV-labeled naive splenic $CD4^+ T_{\text{resp}}$ cells cultured alone or at a ratio of 8:1 with $CD4^+ Foxp3^{EGFP-} T_{\text{conv}}$ suppressor cells (T_{supp}) isolated at day 16 from B16-F10 tumors of DTx-treated $Foxp3^{EGFP}$ -DTR animals. Cells were cultured alone (gray) or with suppressors (purple) along with the indicated reagents. $CD45.2^+ GFP^- T_{\text{supp}}$ suppressor cells were cocultured with 1.25×10^4 suppressor $CD4^+ T_{\text{conv}}$ cells in the presence of 5.0×10^4 APCs. Data are representative of two independently repeated experiments. $n > 3$. P values show significance of difference between no suppressor and suppressor (Student's t test with Bonferroni correction). (B) Representative frequency of dividing T_{resp} cells incubated with tumor $CD4^+ GFP^- T_{\text{conv}}$ cells in the presence of anti-IL-10R antibodies or vehicle. T_{resp} cells without tumor T_{conv} cells were used as a control. (C) Co-correlation between the expression of indicated genes within single-cell gene expression profiles of T cells from tumors of PBS- or DTx-treated B16 tumor-bearing $Foxp3^{EGFP}$ -DTR animals. Pearson correlation coefficient values are indicated by color scale, and genes are hierarchically clustered to identify clusters of coexpressed transcripts within T cell populations. scRNA-Seq data are representative of three biological replicates per group. (D) Measurement of $Ccr8$ and $Iil3$ mRNA expression within $CCR8^-$ and $CCR8^+$ T_{conv} cells from PBS- and DTx-treated animals. Data are representative of three or four biological replicates per group. Ordinary one-way ANOVA, Tukey's multiple comparisons. (E) Tumor area of heterotopic B16-F10 melanoma tumors at indicated time points after implantation into $Il10^{fl/fl} Cd4^{Cre} Foxp3^{EGFP}$ -DTR or $Il10^{+/+} Cd4^{Cre} Foxp3^{EGFP}$ -DTR control mice administered with DTx or PBS from days 10 to 16 after implantation. Data are representative of two independently repeated experiments. $n > 7$, ordinary one-way ANOVA, Tukey's multiple comparisons. (F) Representative histograms (top) and replicate measurements (bottom) of the frequency of $CD8^+ CD44^+$ T cells and $Foxp3^- CD44^+ T_{\text{conv}}$ cells from tumors of animals within indicated treatment groups. (G) Representative frequency and (H) replicate measurements of the frequency (top) and total counts (bottom) of $CD8^+ IFN-\gamma^+ TNF^+$ T cells within tumors. Data are representative of two independently repeated experiments. $n > 4$, one-way ANOVA, Kruskal-Wallis, Dunn's multiple comparisons test. * $P < 0.05$; ** $P < 0.01$; *** $P < 0.001$, **** $P < 0.0001$. Error bars show SEM.

Given these observations, we asked whether CCR8⁺ T_{conv} cells are primary producers of *Il10* mRNA upon depletion of T_{reg} cells. We first examined whether the expression of *Il10* mRNA is co-correlated with the expression of *Ccr8* mRNA, and therefore coexpressed within the same cells, using scRNA-Seq of T cells from tumors of T_{reg} cell-replete and T_{reg} cell-depleted animals. Because IL-10 is known to be produced by CD4⁺ T_{R1} cells that express LAG-3 and CD49b (46–49), Eomes⁺ CD4⁺ T_{conv} cells (50–52), exhausted CD8⁺ T cells that express PD-1 (53), and CD4⁺ T_{H2} cells that express GATA3, IL-4, and IL-13 (54, 55), we included the genes encoding these and other markers in our co-correlation analysis. We found that under steady-state (T_{reg} cell-replete) conditions, *Il10* formed a predominant co-correlation cluster with *Cd8a*, *Pdcdf*, *Ifng*, *Tnf*, and *Eomes* but also a smaller cluster containing *Gata3* and *Foxp3*, suggesting that CD8⁺ T cells in differential states of exhaustion and T_{H2}-like T_{reg} cells are a predominant source of IL-10 (Fig. 6C). However, we found that T_{reg} cell depletion resulted in a striking change in the co-correlation relationship of *Il10* mRNA with the other genes examined, forming a predominant cluster of co-correlated genes containing *Cd4*, *Ccr8*, *Il13*, *Il14*, and *Gata3*. These results suggested that upon T_{reg} cell ablation, the source of *Il10* shifts to the previously identified CD4⁺ CCR8⁺ T_{conv} cell subset with T_{H2}-like characteristics and that CD4⁺ CCR8⁺ T_{conv} cells undergo activation into *Il10*-expressing cells. To confirm this, we sorted CCR8[−] and CCR8⁺ T_{conv} cells from tumors of T_{reg} cell-replete and T_{reg} cell-depleted animals and subjected them to quantitative reverse transcription polymerase chain reaction (qRT-PCR). We found that *Il10* mRNA expression was enriched among CCR8⁺ T_{conv} cells from T_{reg} cell-depleted animals compared with both CCR8[−] cells from T_{reg} cell-depleted animals and CCR8⁺ or CCR8[−] cells from T_{reg} cell-replete animals (Fig. 6D). These findings supported the hypothesis that CCR8⁺ T_{conv} cells become a major source of T cell-expressed IL-10 upon T_{reg} cell depletion.

We therefore asked whether induction of IL-10-dependent suppressive activity among Foxp3[−] T_{conv} cells limits efficacy of T_{reg} cell depletion in vivo. We had observed that T_{reg} cell depletion was ineffective at reducing growth of established B16 tumors, whereas T_{reg} cell depletion during early disease delayed tumor growth but was ineffective at inducing complete responses (Fig. 1A). To test whether IL-10 production by T_{conv} cells is responsible for resistance to T_{reg} cell-depleting therapy in vivo, we generated *Il10*^{flox/flox} *Cd4*^{Cre} *Foxp3*^{EGFP-DTR} (conditionally IL-10-deficient) and littermate *Cd4*^{Cre} *Foxp3*^{EGFP-DTR} (IL-10-proficient) mice. This allowed us to examine the effect of T_{reg} cell depletion in animals whose remaining T cells can or cannot produce IL-10. IL-10 ablation has been shown to promote tumor growth under steady-state conditions (56, 57). We subcutaneously implanted B16-F10 cells into *Il10*^{flox/flox} *Cd4*^{Cre} *Foxp3*^{EGFP-DTR} and littermate *Cd4*^{Cre} *Foxp3*^{EGFP-DTR} control animals and selected animals with tumors of similar size (range, 12 to 64 mm²) at day 10 after tumor implantation for randomization to treatment groups (PBS or DTx). We found that conditional deletion of IL-10 within T cells resulted in loss of resistance to T_{reg} cell depletion, as indicated by reduced tumor growth when T_{reg} cells were ablated in animals lacking T cell-restricted IL-10 expression, but not when either condition was present alone (Fig. 6E). There was also an increase in expression of the activation marker CD44 on CD4⁺ T_{conv} cells and CD8⁺ T cells from animals bearing a conditional deletion of *Il10* and whose T_{reg} cells had been ablated (Fig. 6F). T_{reg} cell ablation in animals bearing a conditional deletion of *Il10* within T cells

was associated with increased frequencies of CD8⁺ T cells and CD4⁺ T_{conv} cells expressing the cytokines interferon-γ (IFN-γ) and tumor necrosis factor (TNF) (Fig. 6, G and H). These results demonstrate a critical role for T cell-produced IL-10 in resistance to T_{reg} cell depletion.

Blockade of IL-10 signaling synergizes with T_{reg} cell depletion to induce robust antitumor immune responses

We next asked whether blockade of IL-10R using anti-IL-10R antibodies reverses resistance to T_{reg} cell-depleting therapy in vivo. We found that late T_{reg} cell depletion or IL-10R blockade alone failed to drive reduction in tumor growth, whereas their combination resulted in tumor regression (Fig. 7A). Moreover, IL-10 blockade synergized with early T_{reg} cell ablation to induce complete responses in a proportion of animals receiving combined therapy (fig. S7). We found that IL-10R blockade both alone and in combination with T_{reg} cell depletion increased the ratio of CD8⁺ T cells expressing IFN-γ and TNF within tumors, but the absolute number of IFN-γ- and TNF-expressing CD8⁺ T cells was markedly increased upon combined T_{reg} cell ablation and IL-10R blockade, reflecting a combination of increased T cell infiltration and cytokine production (Fig. 7, B and C). Similarly, the combination of T_{reg} cell depletion and IL-10R blockade resulted in an increase in the frequency and absolute number of IFN-γ- and TNF-expressing CD4⁺ T cells (Fig. 7, D and E). These findings demonstrate that T_{conv} cells within tumors adopt IL-10-dependent suppressive activity upon therapeutic elimination of T_{reg} cells, contributing to treatment failure of T_{reg} cell-depleting immunotherapies. The findings suggest that combined targeting of T_{reg} cells and compensatory IL-10-dependent suppression invoked upon their depletion may enhance therapy.

DISCUSSION

T_{conv} and T_{reg} cells share components of their activation programs to meet similar metabolic, proliferative, and migratory requirements as they transition from quiescent to activated states (58–60). A substantial effort is now underway to develop therapies that specifically target molecules that distinguish T_{reg} cells within tumors from their T_{conv} cell counterparts. These efforts have been informed by comparative analyses of the molecular profiles of T_{reg} cells and T_{conv} cells within tumors under steady-state conditions (61, 62). We compared the transcriptional profiles of T_{reg} cells with T_{conv} cells not only under steady-state conditions but also upon immune activation provoked by experimental T_{reg} cell ablation. This analysis revealed that T_{conv} cells adopt a highly similar transcriptional profile to T_{reg} cells upon T_{reg} cell depletion. The extent of this reprogramming goes beyond what would be expected as a result of the shared properties of T_{reg} and T_{conv} cell core lymphocyte activation programs and reveals that T_{conv} cells take on compensatory suppressive function when T_{reg} cells are eliminated. Acquisition of a T_{reg} cell-like transcriptional profile by T_{conv} cells upon T_{reg} cell ablation suggests that in practice there are very few molecules whose targeting will enable highly specific depletion of T_{reg} cells within tumors. Nevertheless, a small cluster of genes was identified in our analyses, which has an expression profile limited to T_{reg} cells compared with T_{conv} cells, under both steady-state conditions and upon T_{reg} cell depletion. Although this cluster of genes may contain targets for specific depletion of T_{reg} cells within tumors, a question raised by this study is whether specific

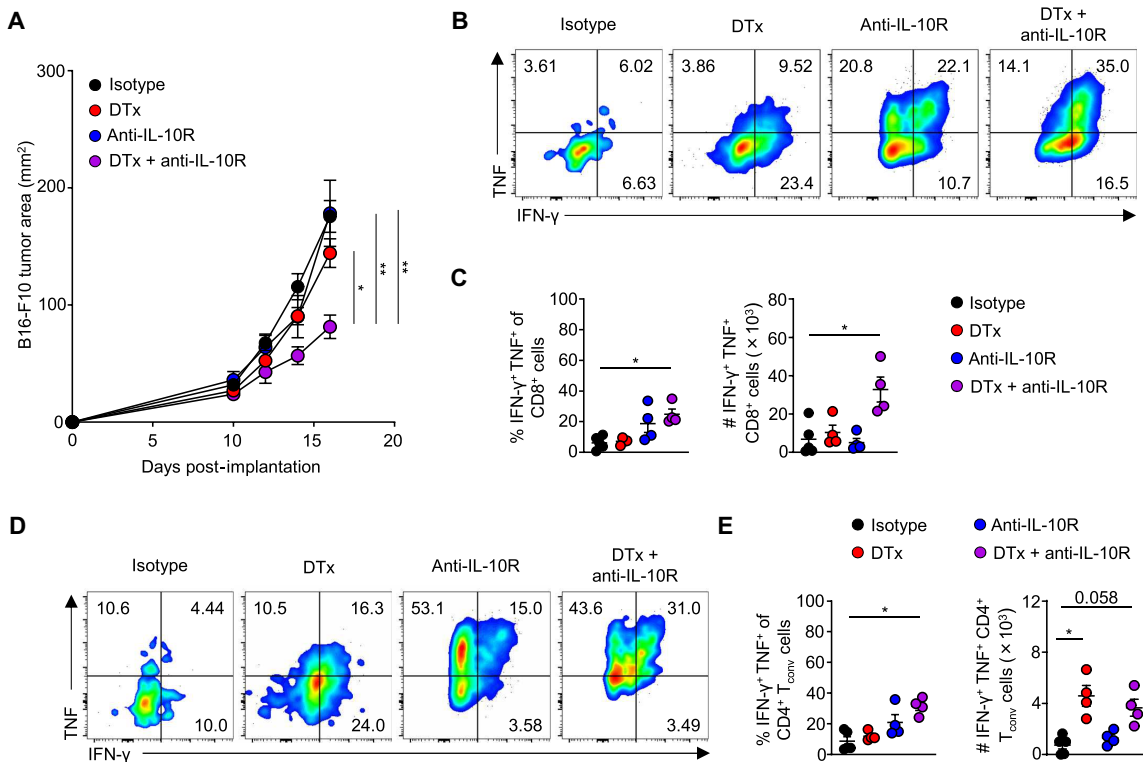


Fig. 7. Blockade of IL-10 signaling synergizes with T_{reg} cell depletion to drive potent antitumor immune responses. (A) Tumor area of B16-F10 melanoma tumors at indicated time points after implantation into *Foxp3*^{EGFP-DTR} animals administered with the indicated combinations of DTx and anti-IL-10R or control reagents from days 10 to 16 after tumor implantation. Data are representative of two independently repeated experiments. $n > 10$, ordinary one-way ANOVA, Tukey's multiple comparisons. * $P < 0.05$, ** $P < 0.01$. (B) Representative frequency and (C) replicate measurements of the frequency and total counts of CD8⁺ IFN- γ + TNF+ T cells from tumors. $n > 3$, one-way ANOVA, Kruskal-Wallis, Dunn's multiple comparisons test, * $P < 0.05$. (D) Representative frequency and (E) replicate measurements of the frequency and total counts of Foxp3⁻ CD4⁺ IFN- γ + TNF+ T cells from tumors. Data are from more than two independent biological replicates. $n > 3$, Kruskal-Wallis, Dunn's multiple comparisons test. * $P < 0.05$. Error bars show SEM.

depletion of T_{reg} cells is desirable rather than the targeting of molecules shared by T_{reg} cells and cells with compensatory suppressive function induced upon T_{reg} cell depletion.

It is known that CCR8 marks highly suppressive T_{reg} cells found in both mouse and human tumors (40–44, 63). There is major interest in the development of therapies that deplete CCR8⁺ T_{reg} cells within tumors. Given our observation that 2CCR8 also marks T_{conv} cells whose suppressive function is induced upon experimental T_{reg} cell ablation in vivo, it is reasonable to postulate that depletion of CCR8-expressing cells is a superior approach to T_{reg} cell depletion using other T_{reg} cell-expressed markers for induction of antitumor immunity, because CCR8-depleting therapies would target both T_{reg} cells and suppressive T_{conv} cells for destruction. It will be important to consider effects of CCR8-depleting therapies on both T_{reg} cells and CCR8⁺ T_{conv} cells within tumors, both in preclinical investigations (42, 63), and whether robust intratumoral depletion of CCR8⁺ cells in the human clinical context is achieved. Alternatively, our data suggest that combining T_{reg} cell-targeted immunotherapies with blockade of IL-10 signaling will overcome compensatory suppression by T_{conv} cells.

It is interesting that the CCR8⁺ T_{conv} cell subset observed in human tumors did not phenotypically overlap with previously described Tr1 cells within tumors. Suppressive Tr1 cells have been characterized in several human tumors including head and neck

squamous cell carcinoma (HNSCC) (64), colorectal cancer (52, 65), hepatocellular carcinoma (49), Hodgkin's lymphoma (66), metastatic melanoma (67), and non-small cell lung cancer (52), and their presence is often associated with tumor progression. The suppressive subset of CCR8⁺ T_{conv} cells we observe does not express EOMES or granzyme K, markers previously reported to be indicative of Tr1 cells. Recent studies have described a contribution of tumor-infiltrating follicular helper T (T_{FH}) cells and follicular regulatory T (T_{FR}) cells to antitumor immunity (68, 69). However, CXCR5 was not expressed by CCR8⁺ T_{conv} cells, suggesting their distinction from T_{FH} cells. We did, however, observe high levels of GATA3 and *Il10* expression among CCR8⁺ T_{conv} cells, suggesting that they represent a T_{H2}-like subset expressing high levels of markers associated with T cell activation, including CD25, which expands systemically and within tumors upon T_{reg} cell depletion. Prior works are consistent with these data, showing systemic expansion of T_{H2} cells expressing either GATA3 or T_{H2} cytokines upon experimental T_{reg} cell ablation (70, 71) and the intratumoral presence of CD4⁺ T_{conv} cells expressing CCR8 (40–44, 63). We found that the frequency of CCR8⁺ CD25⁺ FOXP3⁻ T_{conv} cells inversely correlates with the frequency of tumor-infiltrating CD8⁺ T cells, suggesting that they may play an inhibitory role in human tumor immunity. The observation that CCR8⁺ T_{conv} cells expand and undergo activation to express IL-10 after depletion of T_{reg} cells provides an explanation of

how bulk T_{conv} cells from tumors of T_{reg} cell-depleted animals acquire IL-10-dependent suppressive function despite lack of a change in the relative frequency of CCR8⁺ cells within the tumor CD4⁺ T_{conv} cell compartment. Although our preclinical data from mouse models suggest that CCR8⁺ T_{conv} cells expand numerically within tumors upon experimental T_{reg} cell ablation, this is difficult to formally assess in humans because of the lack of specific markers that are differentially expressed in comparison with FOXP3⁺ T_{reg} cells, enabling their isolation ex vivo, and of clinically approved T_{reg} cell-depleting therapies in widespread use. However, a number of T_{reg} cell-targeted therapies are under development, and it will be an important topic of future investigation to determine their effect upon CCR8⁺ T_{conv} cells in humans. It will also be important to better define how CCR8⁺ T_{conv} cells contribute to immune regulation in other contexts including infection and inflammation, because clones of Foxp3⁻ CD4⁺ T cells co-expressing CCR8, CD25, and IL-10 have previously been described in mice with experimental pulmonary granulomata (72), whereas CD4⁺ T_{conv} cells expressing CCR8 are observed upon experimental allergic lung inflammation in mice (73) and infiltrating human skin (74).

Our findings show that in the context of T_{reg} cell-depleting immunotherapies, IL-10 production by T_{conv} cells represents a secondary layer of immunosuppression responsible for immunotherapy resistance. It is important that this immunosuppressive function of IL-10 in limiting the efficacy of T_{reg} cell-targeted therapies is appreciated, because in other contexts, IL-10 has been shown to have immunostimulatory activity both in preclinical models and in clinical trials (75–77). Our findings suggest that IL-10 blocking antibodies may be used as a synergistic therapy with T_{reg} cell-targeted immunotherapies to improve patient outcomes.

Preclinical studies suggest that T_{reg} cell depletion can reinvigorate T_{conv} cell responses; however, clinical trials of T_{reg} cell-depleting therapies have thus far been met with limited clinical efficacy (35, 78). Although our analysis of human tumor-infiltrating Foxp3⁻ T_{conv} cells revealed a fraction of CCR8⁺ T_{conv} cells under steady-state conditions, it will be valuable to examine whether such cells are expanded upon immunotherapy with either novel T_{reg} cell-depleting therapies or anti-CTLA-4 therapy, the therapeutic efficacy of which is postulated to in part depend on depletion or blockade of the suppressive function of T_{reg} cells (79, 80) and in the context of non-T_{reg} cell-targeted immunotherapy approaches. The prognostic relevance of such cells in determining the outcome of immunotherapy responses will reveal insights into their broader contribution to immunotherapy resistance.

MATERIALS AND METHODS

Study design

The objective of this study was to understand how T_{reg} cell depletion affects the function and immunoregulatory capacity of the T cell lineage in the context of tumor immunity. We used the well-established *Foxp3*^{EGFP-DTR} mouse to experimentally deplete T_{reg} cells in mice with syngeneic B16-F10 melanoma heterotopic tumors. We examined the consequences of T_{reg} cell depletion for tumor progression, as measured by blinded serial caliper measurements and tumor immunity, as assessed by scRNA-Seq and flow cytometry. We found that T_{conv} cells acquire T_{reg} cell-like suppressive functions upon depletion of T_{reg} cells. Using transcriptional profiling and in vitro suppression assays to better understand the nature of this suppressive

activity, we found that suppressive function was enriched among a TH2-like T_{conv} cell subset marked by expression of CCR8. Moreover, using antibody blockade and conditional *Il10* deletion experiments, we found that the suppressive activity induced upon T_{reg} cell depletion was dependent upon IL-10. The sample size for each experiment is specified in the figure legends. The number of independent experiments performed is stated in the figure legends. Age- and sex-matched mice were randomly assigned to each group.

Mice

Foxp3^{EGFP-DTR} mice were originally described by Kim *et al.* (36). *Foxp3*^{IRES-EGFP}, *Ptprc*^a (CD45.1), and *Rag2*^{-/-} mice were obtained from the Jackson Laboratory. *Il10*^{fl/fl} and *Cd4*^{Cre} mice (81) were obtained from J. Langhorne (Francis Crick Institute) and crossed with *Foxp3*^{EGFP-DTR} mice to generate *Il10*^{fl/fl} *Cd4*^{Cre} *Foxp3*^{EGFP-DTR} animals. Experiments were performed using 8- to 14-week-old mice, with age- and sex-matched experimental and control groups. Mice were housed at the University of Cambridge University Biomedical Services (UBS) Gurdon Institute Facility and Babraham Institute Biological Services Unit (BSU). Experiments were conducted in accordance with UK Home Office guidelines and were approved by the University of Cambridge Animal Welfare and Ethics Review Board or by the Babraham Research Campus Animal Welfare and Ethics Review Board.

Human primary tissues

Primary tumors and adjacent healthy tissue were acquired from 48 patients with NSCLC. Patients gave consent to be included in the study, which was approved by the institutional review board of Humanitas Research Hospital (protocol no. 2578). Patients did not receive chemotherapy, radiotherapy, or palliative surgery before samples were obtained. Samples were processed using the gentleMACS Dissociator (Miltenyi Biotec) into single-cell suspensions as previously described (82), resuspended in dimethyl sulfoxide (DMSO) with 10% fetal bovine serum (FBS), and stored in liquid nitrogen.

High-dimensional flow cytometry analysis of human samples and computational processing of flow cytometric data

Samples were prepared for flow cytometry as previously described (82). Panels were developed according to an established protocol (83). Briefly, Flow Cytometry Standard (FCS) 3.0 files were analyzed by standard gating in FlowJo version 9 to remove dead cells and cell aggregates and identify CD4⁺ FOXP3⁻ T cells. Five thousand CD4⁺ FOXP3⁻ T cells per tumor sample (*n* = 48) were subsequently imported into FlowJo (version 10), biexponentially transformed, and exported to be analyzed by a custom-made publicly available pipeline of PhenoGraph (<https://github.com/luglilab/Cytophenograph>). A representative gating strategy is shown in fig. S6. All samples were converted into comma separated value (CSV) files and concatenated in a single matrix by using the merge function of pandas package. The K value, indicating the number of nearest neighbors identified in the first iteration of the algorithm, was set at 500. UMAP was obtained by UMAP Python package.

Tumor challenge and treatment

Mice were injected subcutaneously in the left flank with 1.25×10^5 B16-F10 melanoma cells (American Type Culture Collection). Tumors were measured at serial time points after implantation using

digital calipers, and tumor area was calculated as the product of tumor length and perpendicular width. Tumor measurements were completed by an independent investigator who was not aware of treatment groups or genotypes. For late DTx treatment experiments, mice with tumors between 12 and 64 mm² at day 10 were selected and randomized into treatment groups to reduce experimental variability. Mice were injected intraperitoneally starting at the indicated time point with 1 µg of DTx every other day for a total of four injections and/or 250 µg of anti-IL-10R (clone 1B1.3A; BioXCell) daily for a total of 10 days. DTx from *Corynebacterium diphtheriae* (Sigma-Aldrich) was obtained in lyophilized powder form and reconstituted in sterile double-distilled water according to the manufacturer's instructions.

Suppression assays

The suppressive capacity of tumor T_{conv} cells and T_{reg} cells was measured in vitro as previously described (84). Briefly, CD45.2⁺ TCRβ⁺ CD4⁺ GFP⁺ T_{reg} cells or CD45.2⁺ TCRβ⁺ CD4⁺ GFP⁻ T_{conv} cells were isolated from B16-F10 tumors of *Foxp3*^{EGFP-DTR} mice treated with PBS or DTx using fluorescence-activated cell sorting (FACS) 16 days after implantation and used as suppressor cells. A representative gating strategy is shown in fig. S2. Naïve CD4⁺ T_{conv} cells (CD25⁻ CD44⁻ CD62L⁺) were purified from the spleens of wild-type CD45.1 mice by FACS and stained with CellTrace Violet (CTV) according to the manufacturer's protocol (Thermo Fisher Scientific) and used as responder T (T_{resp}) cells. In total, 2.5 × 10⁴ or 1.25 × 10⁴ (as indicated) suppressor CD4⁺ T_{reg} cells or T_{conv} cells were cocultured with 1 × 10⁵ naïve T_{resp} cells in the presence of anti-CD3 (BioLegend, 1 µg/ml) and 5.0 × 10⁴ *Rag2*^{-/-} antigen-presenting cells (APCs). T_{resp} cells cultured in the presence of anti-CD3 and APCs but without tumor T_{reg} cells or T_{conv} cells were used as a control. Cell division was evaluated by flow cytometry after 4 days of culture. For the screen, cells were cultured alone (gray) or with suppressors (purple) and with aminoglutethimide (AG) at a final concentration of 125 µM or with other indicated reagents at a final concentration of 10 µg/ml.

Flow cytometry of murine samples

Tumor samples were digested using collagenase and deoxyribonuclease for 30 min at 37°C. Percoll was used to isolate lymphocytes from tumors. Tumors and spleens were mechanically dissociated over a 40-µm cell strainer. Red blood cells were lysed using ACK Lysing Buffer (Gibco). Cells were stained with the Fixable Viability Dye eFluor 780 (Thermo Fisher Scientific), Viakrome 808 (Beckman Coulter), or DAPI (4',6-diamidino-2-phenylindole) (Sigma) to discriminate between live and dead cells and then incubated with Fc block (BioXCell, 2.4G2) and combinations of the following surface antibodies for 30 min on ice: anti-TCRβ FITC (fluorescein isothiocyanate) (H57-597), anti-CD8 BV605 (53-6.7), anti-TIM-3 BV421 (RMT3-23), anti-CCR8 BV421 (SA214G2), anti-OX40 BV711 (OX-86), anti-TIGIT PE (phycoerythrin) (4D4/mTIGIT), anti-ICOS BV750 (C398.4A), anti-LAG-3 BV785 (C9B7W), and anti-CD3e Spark Blue 550 (17A2) from BioLegend; anti-CD25 PE-Cyanine7 (PC61.5), anti-CD44 PerCP-Cyanine5.5 (IM7), anti-CD45.1 APC (A20), and anti-CD4 PE-Cy7 (RM4-5) from eBioscience; and anti-GITR BUV805 (DTA-1) and anti-CD4 BUV395 or BUV496 (GK1.5) from BD Biosciences. Cells were stimulated with phorbol 12-myristate 13-acetate (PMA) and ionomycin and blocked with brefeldin A (BFA) for 4 hours in RPMI 1640 complete medium. The intracellular antibodies anti-Foxp3 APC (FJK-16S), anti-IFN-γ

PerCP Cy5.5 (XMG1.2), and anti-GATA3 PE-eFluor610 (TWAJ) were purchased from eBioscience, and anti-CTLA-4 BV605 (UC10-4B9) and anti-TNF PE-Cy7 (MP6-XT22) were purchased from BioLegend and used with the eBioscience Foxp3/Transcription Factor Staining Buffer Set (Invitrogen, Thermo Fisher Scientific) according to the manufacturer's protocol. For determination of CCR8 expression by Foxp3⁻ T_{conv} cells, cells from tumor-bearing *Foxp3*^{EGFP-DTR} animals were surface-stained and analyzed unfixed using flow cytometry, with EGFP expression used to discriminate T_{reg} cells and T_{conv} cells. Samples were analyzed using BD Fortessa, Beckman Coulter CytoFLEX, and Cytek Aurora analyzers. After analysis, data were analyzed using FlowJo software (Tree Star Inc.).

scRNA sequencing and analysis

Single-cell suspensions of T cells were purified by total pan-T cell enrichment (Invitrogen/Thermo Fisher Scientific), and live TCRβ⁺ cells were sorted from B16 tumors by FACS 16 days after implantation. RNA libraries were prepared for scRNA-Seq using the Chromium Single Cell 5' Library & Gel Bead Kit v2 (10x Genomics), processed with Chromium (10x Genomics), and sequenced using the HiSeq 4000 System (Illumina). Raw 10x sequencing data were processed as previously described and mapped to mm10. We confirmed that cells were sequenced to saturation. Data were merged with cell ranger aggr (cellranger-v5.0.0). Merged data were transferred to the R statistical environment for analysis primarily using the package Seurat (v3.2.2) in R v4.0.3. The analysis included only cells expressing between 200 and 2500 genes, <5% mitochondrial-associated transcripts, and genes expressed in at least three cells. The data were then log-normalized and scaled per cell, and variable genes were detected using the FindVariableFeatures function in Seurat, as per default settings, using 2000 features and further processed as per the ScaleData function. Principal components analysis (PCA) was run on the variable genes, and the first six principal components (PCs) were selected for further analyses, based on the SD of the PCs, as determined by an “elbow plot” in Seurat. Cells were clustered using the FindClusters function in Seurat with default settings, resolution = 0.5, and six PCs. UMAP was calculated using six PCs (RunUMAP function). For broadly defining the transcriptional features of each cluster, the FindAllMarkers function (only.pos = FALSE, min.pct = 0.1, thresh.use = 0.2, test.use = “MAST”) was used, and the associated heatmap was generated using the DoHeatmap function using the most uniquely enriched transcripts identified per cluster as defined by FindAllMarkers. The transcriptomic score of a particular cluster was calculated using the AddModuleScore function with default settings. Further visualizations of exported normalized data were generated using the Seurat RidgePlot functions and custom R scripts.

RNA sequencing and analysis

Single-cell suspensions were purified by FACS (as described above) 16 days after tumor implantation and stored in 40 µl of RNAlater Stabilization Solution at -80°C. RNA was extracted from samples using the RNeasy Plus Mini Kit (Qiagen) including the optional QIAshredder step according to the manufacturer's protocol. RNA-Seq analyses were performed using two or more biological replicates. RNA-Seq was performed and analyzed as described previously (59). RNA libraries were prepared using the Clontech SMARTer Ultra Low-input RNA Kit (Takara) and sequenced on an Illumina HiSeq 2500 instrument using Illumina TruSeq v4.0

chemistry. The resulting FastQ files underwent quality control with FastQC, adaptor trimming with Cutadapt, and alignment to the NCBIM37 *Mus musculus* genome annotation with hisat2. Uniquely mapped reads were used to calculate gene expression, and FPM values normalized to total library size with intergenic read normalization were calculated. Differential expression and statistical significance were calculated using the Wald test with adjustment for multiple testing using the Benjamini-Hochberg method and DESeq2 (85). Differentially expressed genes were further analyzed using R. PCA was performed using R plotPCA with count data transformed using variance stabilizing transformation (VST) from fitted dispersion-mean relationships generated using DESeq2 vst. Expression heatmaps were generated using FPM values normalized to row maxima using the R pheatmap package. Hierarchical clustering was performed using the Ward method. Dendograms were cut at levels sufficient to allow two to five clusters to be discriminated.

Statistical analysis

Statistical analysis was performed using GraphPad Prism software. Two-tailed Student's *t* tests or one-way ordinary analyses of variance (ANOVAs) were used unless otherwise indicated to calculate statistical significance of the difference in sample means. *P* values of less than 0.05 were considered statistically significant. Statistical tests used are specified in the figure legends. In all figures, data represent the mean \pm SEM or SD as indicated. *P* values are indicated as follows: ns = not significant, **P* \leq 0.05, ***P* \leq 0.01, ****P* \leq 0.001, *****P* \leq 0.0001.

Supplementary Materials

This PDF file includes:

Figs. S1 to S7

Other Supplementary Material for this manuscript includes the following:

Data files S1 to S6

MDAR Reproducibility Checklist

REFERENCES AND NOTES

1. F. S. Hodi, S. J. O'Day, D. F. McDermott, R. W. Weber, J. A. Sosman, J. B. Haanen, R. Gonzalez, C. Robert, D. Schadendorf, J. C. Hassel, W. Akerley, A. J. van den Eertwegh, J. Lutzky, P. Lorigan, J. M. Vaubel, G. P. Linette, D. Hogg, C. H. Ottensmeier, C. Lebbe, C. Peschel, I. Quirt, J. I. Clark, J. D. Wolchok, J. S. Weber, T. Tian, M. J. Yellin, G. M. Nichol, A. Hoos, W. J. Urba, Improved survival with ipilimumab in patients with metastatic melanoma. *N. Engl. J. Med.* **363**, 711–723 (2010).
2. C. Robert, L. Thomas, I. Bondarenko, S. O'Day, J. Weber, C. Garbe, C. Lebbe, J. F. Baurain, A. Testori, J. J. Grob, N. Davidson, J. Richards, M. Maio, A. Hauschild, W. H. Miller Jr., P. Gascon, M. Lotem, K. Harmankaya, R. Ibrahim, S. Francis, T. T. Chen, R. Humphrey, A. Hoos, J. D. Wolchok, Ipilimumab plus dacarbazine for previously untreated metastatic melanoma. *N. Engl. J. Med.* **364**, 2517–2526 (2011).
3. M. M. Gubin, X. Zhang, H. Schuster, E. Caron, J. P. Ward, T. Noguchi, Y. Ivanova, J. Hundal, C. D. Arthur, W. J. Krebber, G. E. Mulder, M. Toebes, M. D. Vesely, S. S. Lam, A. J. Korman, J. P. Allison, G. J. Freeman, A. H. Sharpe, E. L. Pearce, T. N. Schumacher, R. Aebersold, H. G. Rammensee, C. J. Mielke, E. R. Mardis, W. E. Gillanders, M. N. Artyomov, R. D. Schreiber, Checkpoint blockade cancer immunotherapy targets tumour-specific mutant antigens. *Nature* **515**, 577–581 (2014).
4. J. Larkin, C. D. Lao, W. J. Urba, D. F. McDermott, C. Horak, J. Jiang, J. D. Wolchok, Efficacy and safety of nivolumab in patients with BRAF V600 mutant and BRAF wild-type advanced melanoma: A pooled analysis of 4 clinical trials. *JAMA Oncol.* **1**, 433–440 (2015).
5. J. Larkin, V. Chiarion-Sileni, R. Gonzalez, J. J. Grob, C. L. Cowey, C. D. Lao, D. Schadendorf, R. Dummer, M. Smylie, P. Rutkowski, P. F. Ferrucci, A. Hill, J. Wagstaff, M. S. Carlino, J. B. Haanen, M. Maio, I. Marquez-Rodas, G. A. McArthur, P. A. Ascierto, G. V. Long, M. K. Callahan, M. A. Postow, K. Grossmann, M. Szoln, B. Dreno, L. Bastholt, A. Yang, L. M. Rollin, C. Horak, F. S. Hodi, J. D. Wolchok, Combined nivolumab and ipilimumab or monotherapy in untreated melanoma. *N. Engl. J. Med.* **373**, 23–34 (2015).
6. P. Sharma, S. Hu-Lieskovian, J. A. Wargo, A. Ribas, Primary, adaptive, and acquired resistance to cancer immunotherapy. *Cell* **168**, 707–723 (2017).
7. M. Reck, D. Rodriguez-Abreu, A. G. Robinson, R. Hui, T. Csoszi, A. Fulop, M. Gottfried, N. Peled, A. Tafreshi, S. Cuffe, M. O'Brien, S. Rao, K. Hotta, M. A. Leiby, G. M. Lubiniecki, Y. Shentu, R. Rangwala, J. R. Brahmer; KEYNOTE-024 Investigators, Pembrolizumab versus chemotherapy for PD-L1-positive non-small-cell lung cancer. *N. Engl. J. Med.* **375**, 1823–1833 (2016).
8. O. Hamid, L. Molinero, C. R. Bolen, J. A. Sosman, E. Munoz-Couselo, H. M. Kluger, D. F. McDermott, J. D. Powderly, I. Sarkar, M. Ballinger, M. Fasso, C. O'Hear, D. S. Chen, P. S. Hegde, F. S. Hodi, Safety, clinical activity, and biological correlates of response in patients with metastatic melanoma: Results from a phase I trial of atezolizumab. *Clin. Cancer Res.* **25**, 6061–6072 (2019).
9. G. Plitas, A. Y. Rudensky, Regulatory T cells in cancer. *Annu. Rev. Cancer Biol.* **4**, 459–477 (2020).
10. K. DePauw, G. M. Delgoffe, Metabolic barriers to cancer immunotherapy. *Nat. Rev. Immunol.* **21**, 785–797 (2021).
11. S. Sakaguchi, N. Mikami, J. B. Wing, A. Tanaka, K. Ichiyama, N. Ohkura, Regulatory T cells and human disease. *Annu. Rev. Immunol.* **38**, 541–566 (2020).
12. A. Gallimore, S. A. Quezada, R. Roychoudhuri, Regulatory T cells in cancer: Where are we now? *Immunology* **157**, 187–189 (2019).
13. J. Stockis, R. Roychoudhuri, T. Y. F. Halim, Regulation of regulatory T cells in cancer. *Immunology* **157**, 219–231 (2019).
14. R. Roychoudhuri, R. L. Eil, N. P. Restifo, The interplay of effector and regulatory T cells in cancer. *Curr. Opin. Immunol.* **33**, 101–111 (2015).
15. E. Sato, S. H. Olson, J. Ahn, B. Bundy, H. Nishikawa, F. Qian, A. A. Jungbluth, D. Frosina, S. Gnajatic, C. Ambrosone, J. Kepner, T. Odunsi, G. Ritter, S. Lele, Y. T. Chen, H. Ohtani, L. J. Old, K. Odunsi, Intraepithelial CD8+ tumor-infiltrating lymphocytes and a high CD8+/regulatory T cell ratio are associated with favorable prognosis in ovarian cancer. *Proc. Natl. Acad. Sci. U.S.A.* **102**, 18538–18543 (2005).
16. T. J. Curiel, G. Coukos, L. Zou, X. Alvarez, P. Cheng, P. Mottram, M. Evdemon-Hogan, J. R. Conejo-Garcia, L. Zhang, M. Burow, Y. Zhu, S. Wei, I. Kryczek, B. Daniel, A. Gordon, L. Myers, A. Lackner, M. L. Disis, K. L. Knutson, L. Chen, W. Zou, Specific recruitment of regulatory T cells in ovarian carcinoma fosters immune privilege and predicts reduced survival. *Nat. Med.* **10**, 942–949 (2004).
17. G. J. Bates, S. B. Fox, C. Han, R. D. Leek, J. F. Garcia, A. L. Harris, A. H. Banham, Quantification of regulatory T cells enables the identification of high-risk breast cancer patients and those at risk of late relapse. *J. Clin. Oncol.* **24**, 5373–5380 (2006).
18. R. P. Petersen, M. J. Campa, J. Sperlazzia, D. Conlon, M. B. Joshi, D. H. Harpole Jr., E. F. Patz Jr., Tumor infiltrating Foxp3+ regulatory T-cells are associated with recurrence in pathologic stage I NSCLC patients. *Cancer* **107**, 2866–2872 (2006).
19. Q. Gao, S. J. Qiu, J. Fan, J. Zhou, X. Y. Wang, Y. S. Xiao, Y. Xu, Y. W. Li, Z. Y. Tang, Intratumoral balance of regulatory and cytotoxic T cells is associated with prognosis of hepatocellular carcinoma after resection. *J. Clin. Oncol.* **25**, 2586–2593 (2007).
20. R. W. Griffiths, E. Elkord, D. E. Gilham, V. Ramani, N. Clarke, P. L. Stern, R. E. Hawkins, Frequency of regulatory T cells in renal cell carcinoma patients and investigation of correlation with survival. *Cancer Immunol. Immunother.* **56**, 1743–1753 (2007).
21. N. Hiraoka, K. Onozato, T. Kosuge, S. Hirohashi, Prevalence of FOXP3+ regulatory T cells increases during the progression of pancreatic ductal adenocarcinoma and its premalignant lesions. *Clin. Cancer Res.* **12**, 5423–5434 (2006).
22. G. Perrone, P. A. Ruffini, V. Catalano, C. Spino, D. Santini, P. Muretto, C. Spoto, C. Zingaretti, V. Sisti, P. Alessandroni, P. Giordani, A. Cicetti, S. D'Emidio, S. Morini, A. Ruzzo, M. Magnani, G. Tonini, C. Rabitti, F. Graziano, Intratumoural FOXP3-positive regulatory T cells are associated with adverse prognosis in radically resected gastric cancer. *Eur. J. Cancer* **44**, 1875–1882 (2008).
23. E. S. Jordanova, A. Gorter, O. Ayachi, F. Prins, L. G. Durrant, G. G. Kenter, S. H. van der Burg, G. J. Fleuren, Human leukocyte antigen class I, MHC class I chain-related molecule A, and CD8+/regulatory T-cell ratio: Which variable determines survival of cervical cancer patients? *Clin. Cancer Res.* **14**, 2028–2035 (2008).
24. G. Alvisi, A. Termanini, C. Soldani, F. Portale, R. Carriero, K. Pilipow, G. Costa, M. Polidoro, B. Franceschini, I. Malenica, S. Puccio, V. Lise, G. Galletti, V. Zanon, F. S. Colombo, G. De Simone, M. Tufano, A. Aghemo, L. Di Tommaso, C. Peano, J. Cibella, M. Iannaccone, R. Roychoudhuri, T. Manzo, M. Donadon, G. Torzilli, P. Kunderfranco, D. Di Mitri, E. Lugli, A. Leo, Multimodal single-cell profiling of intrahepatic cholangiocarcinoma defines hyperactivated Tregs as a potential therapeutic target. *J. Hepatol.* **77**, 1359–1372 (2022).
25. F. A. Sinicrope, R. L. Rego, S. M. Anselli, K. L. Knutson, N. R. Foster, D. J. Sargent, Intraepithelial effector (CD3+)/regulatory (FoxP3+) T-cell ratio predicts a clinical outcome of human colon carcinoma. *Gastroenterology* **137**, 1270–1279 (2009).
26. T. Maj, W. Wang, J. Crespo, H. Zhang, W. Wang, S. Wei, L. Zhao, L. Vatan, I. Shao, W. Szeliga, C. Lyskiotis, J. R. Liu, I. Kryczek, W. Zou, Oxidative stress controls regulatory T cell apoptosis and suppressor activity and PD-L1-blockade resistance in tumor. *Nat. Immunol.* **18**, 1332–1341 (2017).
27. T. R. Simpson, F. Li, W. Montalvo-Ortiz, M. A. Sepulveda, K. Bergerhoff, F. Arce, C. Roddie, J. Y. Henry, H. Yagita, J. D. Wolchok, K. S. Peggs, J. V. Ravetch, J. P. Allison, S. A. Quezada,

- Fc-dependent depletion of tumor-infiltrating regulatory T cells co-defines the efficacy of anti-CTLA-4 therapy against melanoma. *J. Exp. Med.* **210**, 1695–1710 (2013).
28. P. Yu, Y. Lee, W. Liu, T. Krausz, A. Chong, H. Schreiber, Y. X. Fu, Intratumor depletion of CD4+ cells unmasks tumor immunogenicity leading to the rejection of late-stage tumors. *J. Exp. Med.* **201**, 779–791 (2005).
 29. C. Liu, C. J. Workman, D. A. Vignali, Targeting regulatory T cells in tumors. *FEBS J.* **283**, 2731–2748 (2016).
 30. J. F. Jacobs, C. J. Punt, W. J. Lesterhuis, R. P. Sutmuller, H. M. Brouwer, N. M. Scharenborg, I. S. Klasen, L. B. Hilbrands, C. G. Figgdr, I. J. de Vries, G. J. Adema, Dendritic cell vaccination in combination with anti-CD25 monoclonal antibody treatment: A phase I/II study in metastatic melanoma patients. *Clin. Cancer Res.* **16**, 5067–5078 (2010).
 31. J. H. Sampson, R. J. Schmittling, G. E. Archer, K. L. Congdon, S. K. Nair, E. A. Reap, A. Desjardins, A. H. Friedman, H. S. Friedman, J. E. Herndon 2nd, A. Coan, R. E. McLendon, D. A. Reardon, J. J. Vredenburgh, D. D. Bigner, D. A. Mitchell, A pilot study of IL-2R α blockade during lymphopenia depletes regulatory T-cells and correlates with enhanced immunity in patients with glioblastoma. *PLOS ONE* **7**, e31046 (2012).
 32. A. J. Rech, R. Mick, S. Martin, A. Recio, N. A. Aqui, D. J. Powell Jr., T. A. Colligon, J. A. Trosko, L. I. Leinbach, C. H. Pletcher, C. K. Tweed, A. DeMichele, K. R. Fox, S. M. Domchek, J. L. Riley, R. H. Vonderheide, CD25 blockade depletes and selectively reprograms regulatory T cells in concert with immunotherapy in cancer patients. *Sci. Transl. Med.* **4**, 134ra162 (2012).
 33. P. Attia, A. V. Maker, L. R. Haworth, L. Rogers-Freezer, S. A. Rosenberg, Inability of a fusion protein of IL-2 and diphtheria toxin (Denileukin Diftitox, DAB389IL-2, ONTAK) to eliminate regulatory T lymphocytes in patients with melanoma. *J. Immunother.* **28**, 582–592 (2005).
 34. D. Zamarin, O. Hamid, A. Nayak-Kapoor, S. Sahebjam, M. Szolnok, A. Collaku, F. E. Fox, M. A. Marshall, D. S. Hong, Mogamulizumab in combination with durvalumab or tremelimumab in patients with advanced solid tumors: A phase I study. *Clin. Cancer Res.* **26**, 4531–4541 (2020).
 35. K. Kurose, Y. Ohue, H. Wada, S. Iida, T. Ishida, T. Kojima, T. Doi, S. Suzuki, M. Isobe, T. Funakoshi, K. Kakimi, H. Nishikawa, H. Udon, M. Oka, R. Ueda, E. Nakayama, Phase Ia study of FoxP3+ CD4 Treg depletion by infusion of a humanized anti-CCR4 antibody, KW-0761, in cancer patients. *Clin. Cancer Res.* **21**, 4327–4336 (2015).
 36. J. M. Kim, J. P. Rasmussen, A. Y. Rudensky, Regulatory T cells prevent catastrophic autoimmunity throughout the lifespan of mice. *Nat. Immunol.* **8**, 191–197 (2007).
 37. T. Takahashi, Y. Kuniyasu, M. Toda, N. Sakaguchi, M. Itoh, M. Iwata, J. Shimizu, S. Sakaguchi, Immunologic self-tolerance maintained by CD25+CD4+ naturally anergic and suppressive T cells: Induction of autoimmune disease by breaking their anergic/suppressive state. *Int. Immunol.* **10**, 1969–1980 (1998).
 38. L. W. Collison, M. R. Pillai, V. Chaturvedi, D. A. Vignali, Regulatory T cell suppression is potentiated by target T cells in a cell contact, IL-35- and IL-10-dependent manner. *J. Immunol.* **182**, 6121–6128 (2009).
 39. A. M. Thornton, E. M. Shevach, CD4+CD25+ immunoregulatory T cells suppress polyclonal T cell activation in vitro by inhibiting interleukin 2 production. *J. Exp. Med.* **188**, 287–296 (1998).
 40. D. O. Villarreal, A. L'Huillier, S. Armington, C. Mottershead, E. V. Filippova, B. D. Coder, R. G. Petit, M. F. Princiotta, Targeting CCR8 induces protective antitumor immunity and enhances vaccine-induced responses in colon cancer. *Cancer Res.* **78**, 5340–5348 (2018).
 41. S. K. Whiteside, F. M. Grant, D. S. Gyori, A. G. Conti, C. J. Imianowski, P. Kuo, R. Nasrallah, F. Sadiyah, S. A. Lira, F. Tacke, R. L. Eil, O. T. Burton, J. Dooley, A. Liston, K. Okkenhaug, J. Yang, R. Roychoudhuri, CCR8 marks highly suppressive Treg cells within tumors but is dispensable for their accumulation and suppressive function. *Immunity* **163**, 512–520 (2021).
 42. H. Van Damme, B. Dombrecht, M. Kiss, H. Roose, E. Allen, E. Van Overmeire, D. Kancheva, L. Martens, A. Murgaski, P. M. R. Bardet, G. Blancke, M. Jans, E. Bolli, M. S. Martins, Y. Elkrim, J. Dooley, L. Boon, J. K. Schwarze, F. Tacke, K. Movahedi, N. Vandamme, B. Neyns, S. Ocak, I. Scheyltjens, L. Vereecke, F. A. Nana, P. Merchiers, D. Laoui, J. A. Van Ginderachter, Therapeutic depletion of CCR8 $^{+}$ tumor-infiltrating regulatory T cells elicits antitumor immunity and synergizes with anti-PD-1 therapy. *J. Immunother. Cancer* **9**, e001749 (2021).
 43. J. R. Campbell, B. R. McDonald, P. B. Mesko, N. O. Siemers, P. B. Singh, M. Selby, T. W. Sproul, A. J. Korman, L. M. Vlach, J. Houser, S. Sambanthamoorthy, K. Lu, S. V. Hatcher, J. Lohre, R. Jain, R. Y. Lan, Fc-optimized anti-CCR8 antibody depletes regulatory T cells in human tumor models. *Cancer Res.* **81**, 2983–2994 (2021).
 44. G. Alvisi, J. Brummelman, S. Puccio, E. M. Mazza, E. P. Tomada, A. Losurdo, V. Zanon, C. Peano, F. S. Colombo, A. Scarpa, M. Alloisio, A. Vasanthakumar, R. Roychoudhuri, M. Kallikourdis, M. Pagani, E. Lopci, P. Novellis, J. Blume, A. Kallies, G. Veronesi, E. Lugli, IRF4 instructs effector Treg differentiation and immune suppression in human cancer. *J. Clin. Invest.* **130**, 3137–3150 (2020).
 45. B. Mahata, J. Pramanik, L. van der Weyden, K. Polanski, G. Kar, A. Riedel, X. Chen, N. A. Fonseca, K. Kundu, L. S. Campos, E. Ryder, G. Duddy, I. Walczak, K. Okkenhaug, D. J. Adams, J. D. Shields, S. A. Teichmann, Tumors induce de novo steroid biosynthesis in T cells to evade immunity. *Nat. Commun.* **11**, 3588 (2020).
 46. H. Groux, A. O'Garra, M. Bigler, M. Rouleau, S. Antonenko, J. E. de Vries, M. G. Roncarolo, A CD4+ T-cell subset inhibits antigen-specific T-cell responses and prevents colitis. *Nature* **389**, 737–742 (1997).
 47. M. G. Roncarolo, H. Yssel, J. L. Touraine, H. Betuel, J. E. De Vries, H. Spits, Autoreactive T cell clones specific for class I and class II HLA antigens isolated from a human chimera. *J. Exp. Med.* **167**, 1523–1534 (1988).
 48. N. Gagliani, C. F. Magnani, S. Huber, M. E. Gianolini, M. Pala, P. Licona-Limon, B. Guo, D. R. Herbert, A. Bulfone, F. Trentini, C. Di Serio, R. Bacchetta, M. Andreani, L. Brockmann, S. Gregori, R. A. Flavell, M. G. Roncarolo, Coexpression of CD49b and LAG-3 identifies human and mouse T regulatory type 1 cells. *Nat. Med.* **19**, 739–746 (2013).
 49. A. Pedroza-Gonzalez, G. Zhou, E. Vargas-Mendez, P. P. Boor, S. Mancham, C. Verhoef, W. G. Polak, D. Grunhagen, Q. Pan, H. Janssen, G. S. Garcia-Romo, K. Biermann, E. T. Tjwa, E. T. Tjwa, J. N. IJzermans, J. Kwekkeboom, D. Sprengers, Tumor-infiltrating plasmacytoid dendritic cells promote immunosuppression by Tr1 cells in human liver tumors. *Oncotargets Ther.* **4**, e1008355 (2015).
 50. P. Zhang, J. S. Lee, K. H. Gartlan, I. S. Schuster, I. Comerford, A. Varelias, M. A. Ullah, S. Vuckovic, M. Koyama, R. D. Kuns, K. R. Locke, K. J. Beckett, S. D. Olver, L. D. Samson, M. Montes de Oca, F. de Labastida Rivera, A. D. Clouston, G. T. Belz, B. R. Blazquez, K. P. MacDonald, S. R. McColl, R. Thomas, C. R. Engwerda, M. A. Degli-Esposti, A. Kallies, S. K. Tey, G. R. Hill, Eomesodermin promotes the development of type 1 regulatory T (T_{R1}) cells. *Sci. Immunol.* **2**, eaah7152 (2017).
 51. P. Gruarin, S. Maglie, M. De Simone, B. Haringer, C. Vasco, V. Ranzani, R. Bosotti, J. S. Noddings, P. Larghi, F. Facciotti, M. L. Sarnicola, M. Martinovic, M. Crosti, M. Moro, R. L. Rossi, M. E. Bernardo, F. Caprioli, F. Locatelli, G. Rossetti, S. Abrignani, M. Pagani, J. Geginat, Eomesodermin controls a unique differentiation program in human IL-10 and IFN- γ coproducing regulatory T cells. *Eur. J. Immunol.* **49**, 96–111 (2019).
 52. R. J. P. Bonnal, G. Rossetti, E. Lugli, M. De Simone, P. Gruarin, J. Brummelman, L. Drufuca, M. Passaro, R. Bason, F. Gervasoni, G. D. Chiara, C. D'Oria, M. Martinovic, S. Curti, V. Ranzani, C. Cordigliero, G. Alvisi, E. M. C. Mazza, S. Oliveto, Y. Silvestri, E. Carelli, S. Mazzara, R. Bosotti, M. L. Sarnicola, C. Godano, V. Bevilacqua, M. Lorenzo, S. Siena, E. Bonoldi, A. Sartore-Bianchi, A. Amato, G. Veronesi, P. Novellis, M. Alloisio, A. Gianni, N. Zucchini, E. Opocher, A. P. Ceretti, N. Mariani, S. Biffo, D. Prati, A. Bardelli, J. Geginat, A. Lanzavecchia, S. Abrignani, M. Pagani, Clonally expanded EOMES $^{+}$ Tr1-like cells in primary and metastatic tumors are associated with disease progression. *Nat. Immunol.* **22**, 735–745 (2021).
 53. H. T. Jin, A. C. Anderson, W. G. Tan, E. E. West, S. J. Ha, K. Araki, G. J. Freeman, V. K. Kuchroo, R. Ahmed, Cooperation of Tim-3 and PD-1 in CD8 T-cell exhaustion during chronic viral infection. *Proc. Natl. Acad. Sci. U.S.A.* **107**, 14733–14738 (2010).
 54. D. F. Fiorentino, M. W. Bond, T. R. Mosmann, Two types of mouse T helper cell. IV. Th2 clones secrete a factor that inhibits cytokine production by Th1 clones. *J. Exp. Med.* **170**, 2081–2095 (1989).
 55. K. W. Moore, R. de Waal Malefyt, R. L. Coffman, A. O'Garra, Interleukin-10 and the interleukin-10 receptor. *Annu. Rev. Immunol.* **19**, 683–765 (2001).
 56. T. Tanikawa, C. M. Wilke, I. Kryczek, G. Y. Chen, J. Kao, G. Nunez, W. Zou, Interleukin-10 ablation promotes tumor development, growth, and metastasis. *Cancer Res.* **72**, 420–429 (2012).
 57. E. Pastille, K. Bardini, D. Fleissner, A. Adamczyk, A. Frede, M. Wadwa, D. von Smolinski, S. Kasper, T. Sparwasser, A. D. Gruber, M. Schuler, S. Sakaguchi, A. Roers, W. Muller, W. Hansen, J. Buer, A. M. Westendorf, Transient ablation of regulatory T cells improves antitumor immunity in colitis-associated colon cancer. *Cancer Res.* **74**, 4258–4269 (2014).
 58. F. M. Grant, J. Yang, R. Nasrallah, J. Clarke, F. Sadiyah, S. K. Whiteside, C. J. Imianowski, P. Kuo, P. Vardaka, T. Todorov, N. Zandhuis, I. Patrascu, D. F. Tough, K. Kometani, R. Eil, T. Kurosaki, K. Okkenhaug, R. Roychoudhuri, BACH2 drives quiescence and maintenance of resting Treg cells to promote homeostasis and cancer immunosuppression. *J. Exp. Med.* **217**, e20190711 (2020).
 59. R. Roychoudhuri, D. Clever, P. Li, Y. Wakabayashi, K. M. Quinn, C. A. Klebanoff, Y. Ji, M. Sukumar, R. L. Eil, Z. Yu, R. Spolski, D. C. Palmer, J. H. Pan, S. J. Patel, D. C. Macallan, G. Fabozzi, H. Y. Shih, Y. Kanno, A. Muto, J. Zhu, L. Gattinoni, J. J. O'Shea, K. Okkenhaug, K. Igarashi, W. J. Leonard, N. P. Restifo, BACH2 regulates CD8 $^{+}$ T cell differentiation by controlling access of AP-1 factors to enhancers. *Nat. Immunol.* **17**, 851–860 (2016).
 60. K. Igarashi, T. Kurosaki, R. Roychoudhuri, BACH transcription factors in innate and adaptive immunity. *Nat. Rev. Immunol.* **17**, 437–450 (2017).
 61. M. De Simone, A. Arrigoni, G. Rossetti, P. Gruarin, V. Ranzani, C. Politano, R. J. P. Bonnal, E. Provasi, M. L. Sarnicola, I. Panzeri, M. Moro, M. Crosti, S. Mazzara, V. Vaira, S. Bosari, A. Palleschi, L. Santambrogio, G. Bovo, N. Zucchini, M. Totis, L. Gianotti, G. Cesana, R. A. Perego, N. Maroni, A. P. Ceretti, E. Opocher, R. De Francesco, J. Geginat, H. G. Stunnenberg, S. Abrignani, M. Pagani, Transcriptional landscape of human tissue lymphocytes unveils uniqueness of tumor-infiltrating T regulatory cells. *Immunity* **45**, 1135–1147 (2016).
 62. G. Plitas, C. Konopacki, K. Wu, P. D. Bos, M. Morrow, E. V. Putintseva, D. M. Chudakov, A. Y. Rudensky, Regulatory T cells exhibit distinct features in human breast cancer. *Immunity* **45**, 1122–1134 (2016).
 63. Y. Kidani, W. Nogami, Y. Yasumizu, A. Kawashima, A. Tanaka, Y. Sonoda, Y. Tona, K. Nashiki, R. Matsumoto, M. Hagiwara, M. Osaki, K. Dohi, T. Kanazawa, A. Ueyama, M. Yoshikawa, T. Yoshida, M. Matsumoto, K. Hojo, S. Shinonome, H. Yoshida, M. Hirata, M. Haruna,

- Y. Nakamura, D. Motooka, D. Okuzaki, Y. Sugiyama, M. Kinoshita, T. Okuno, T. Kato, K. Hatano, M. Uemura, R. Imamura, K. Yokoi, A. Tanemura, Y. Shintani, T. Kimura, N. Nonomura, H. Wada, M. Mori, Y. Doki, N. Ohkura, S. Sakaguchi, CCR8-targeted specific depletion of clonally expanded Treg cells in tumor tissues evokes potent tumor immunity with long-lasting memory. *Proc. Natl. Acad. Sci. U.S.A.* **119**, e2114282119 (2022).
64. C. Bergmann, L. Strauss, Y. Wang, M. J. Szczepanski, S. Lang, J. T. Johnson, T. L. Whiteside, T regulatory type 1 cells in squamous cell carcinoma of the head and neck: Mechanisms of suppression and expansion in advanced disease. *Clin. Cancer Res.* **14**, 3706–3715 (2008).
65. M. Scurr, K. Ladell, M. Besneux, A. Christian, T. Hockey, K. Smart, H. Bridgeman, R. Hargest, S. Phillips, M. Davies, D. Price, A. Gallimore, A. Godkin, Highly prevalent colorectal cancer-infiltrating LAP⁺ Foxp3⁺ T cells exhibit more potent immunosuppressive activity than Foxp3⁺ regulatory T cells. *Mucosal Immunol.* **7**, 428–439 (2014).
66. N. A. Marshall, L. E. Christie, L. R. Munro, D. J. Culligan, P. W. Johnston, R. N. Barker, M. A. Vickery, Immunosuppressive regulatory T cells are abundant in the reactive lymphocytes of Hodgkin lymphoma. *Blood* **103**, 1755–1762 (2004).
67. H. Yan, P. Zhang, X. Kong, X. Hou, L. Zhao, T. Li, X. Yuan, H. Fu, Primary Tr1 cells from metastatic melanoma eliminate tumor-promoting macrophages through granzyme B- and perforin-dependent mechanisms. *Tumour Biol.* **39**, 1010428317697554 (2017).
68. R. Zappasodi, S. Budhu, M. D. Hellmann, M. A. Postow, Y. Senbabaoglu, S. Manne, B. Gasmi, C. Liu, H. Zhong, Y. Li, A. C. Huang, D. Hirschhorn-Cymerman, K. S. Panageas, E. J. Wherry, T. Merghoub, J. D. Wolchok, Non-conventional inhibitory CD4⁺Foxp3⁺PD-1^{hi} T cells as a biomarker of immune checkpoint blockade activity. *Cancer Cell* **33**, 1017–1032.e7 (2018).
69. S. Eschweiler, J. Clarke, C. Ramirez-Suastegui, B. Panwar, A. Madrigal, S. J. Chee, I. Karydis, E. Woo, A. Alzatani, S. Elsheikh, C. J. Hanley, G. J. Thomas, P. S. Friedmann, T. Sanchez-Elsner, F. Ay, C. H. Ottensmeier, P. Vijayanand, Intratumoral follicular regulatory T cells curtail anti-PD-1 treatment efficacy. *Nat. Immunol.* **22**, 1052–1063 (2021).
70. K. Lahl, C. T. Mayer, T. Bopp, J. Huehn, C. Loddenkemper, G. Eberl, G. Wirsberger, K. Dornmair, R. Geffers, E. Schmitt, J. Buer, T. Sparwasser, Nonfunctional regulatory T cells and defective control of Th2 cytokine production in natural scurfy mutant mice. *J. Immunol.* **183**, 5662–5672 (2009).
71. L. Tian, J. A. Altin, L. E. Makaroff, D. Franckaert, M. C. Cook, C. C. Goodnow, J. Dooley, A. Liston, Foxp3⁺ regulatory T cells exert asymmetric control over murine helper responses by inducing Th2 cell apoptosis. *Blood* **118**, 1845–1853 (2011).
72. C. M. Freeman, B. C. Chiu, V. R. Stolberg, J. Hu, K. Zeibecoglou, N. W. Lukacs, S. A. Lira, S. L. Kunkel, S. W. Chensue, CCR8 is expressed by antigen-elicited, IL-10-producing CD4+CD25+T cells, which regulate Th2-mediated granuloma formation in mice. *J. Immunol.* **174**, 1962–1970 (2005).
73. Z. Mikhak, M. Fukui, A. Farsidjani, B. D. Medoff, A. M. Tager, A. D. Luster, Contribution of CCR4 and CCR8 to antigen-specific T(H)2 cell trafficking in allergic pulmonary inflammation. *J. Allergy Clin. Immunol.* **123**, 67–73.e3 (2009).
74. M. L. McCully, K. Ladell, R. Andrews, R. E. Jones, K. L. Miners, L. Roger, D. M. Baird, M. J. Cameron, Z. M. Jessop, I. S. Whitaker, E. L. Davies, D. A. Price, B. Moser, CCR8 expression defines tissue-resident memory T cells in human skin. *J. Immunol.* **200**, 1639–1650 (2018).
75. Y. Guo, Y. Q. Xie, M. Gao, Y. Zhao, F. Franco, M. Wenes, I. Siddiqui, A. Bevilacqua, H. Wang, H. Yang, B. Feng, X. Xie, C. M. Sabatel, B. Tscharn, A. Chaiboonchoe, Y. Wang, W. Li, W. Xiao, W. Held, P. Romero, P. C. Ho, L. Tang, Metabolic reprogramming of terminally exhausted CD8⁺ T cells by IL-10 enhances anti-tumor immunity. *Nat. Immunol.* **22**, 746–756 (2021).
76. A. Naing, J. R. Infante, K. P. Papadopoulos, I. H. Chan, C. Shen, N. P. Ratti, B. Rojo, K. A. Autio, D. J. Wong, M. R. Patel, P. A. Ott, G. S. Falchook, S. Pant, A. Hung, K. L. Pekarek, V. Wu, M. Adamow, S. McCauley, J. B. Mumma, P. Wong, P. Van Vlasselaer, J. Leveque, N. M. Tannir, M. Oft, PEGylated IL-10 (peglolodecakin) induces systemic immune activation, CD8⁺ T cell invigoration and polyclonal T cell expansion in cancer patients. *Cancer Cell* **34**, 775–791.e773 (2018).
77. N. M. Tannir, K. P. Papadopoulos, D. J. Wong, R. Aljumaily, A. Hung, M. Afable, J. S. Kim, D. Ferry, A. Drakaki, J. Bendell, A. Naing, Pegilodecakin as monotherapy or in combination with anti-PD-1 or tyrosine kinase inhibitor in heavily pretreated patients with advanced renal cell carcinoma: Final results of cohorts A, G, H and I of IVY Phase I study. *Int. J. Cancer* **149**, 403–408 (2021).
78. B. S. Glisson, R. S. Leidner, R. L. Ferris, J. Powderly, N. A. Rizvi, B. Keam, R. Schneider, S. Goel, J. P. Ohr, J. Burton, Y. Zheng, S. Eck, M. Grubin, K. Streicher, D. M. Townsley, S. P. Patel, Safety and clinical activity of MED10562, a humanized OX40 agonist monoclonal antibody, in adult patients with advanced solid tumors. *Clin. Cancer Res.* **26**, 5358–5367 (2020).
79. E. Romano, M. Kusio-Kobialka, P. G. Foukas, P. Baumgaertner, C. Meyer, P. Ballabeni, O. Michelin, B. Weide, P. Romero, D. E. Speiser, Ipilimumab-dependent cell-mediated cytotoxicity of regulatory T cells ex vivo by nonclassical monocytes in melanoma patients. *Proc. Natl. Acad. Sci. U.S.A.* **112**, 6140–6145 (2015).
80. F. Arce Vargas, A. J. S. Furness, K. Litchfield, K. Joshi, R. Rosenthal, E. Ghorani, I. Solomon, M. H. Lesko, N. Ruef, C. Roddie, J. Y. Henry, L. Spain, A. Ben Aissa, A. Georgiou, Y. N. S. Wong, M. Smith, D. Strauss, A. Hayes, D. Nicol, T. O'Brien, L. Martensson, A. Ljungars, I. Teige, B. Frendeus, T. R. Melanoma, T. R. Renal, T. R. L. Consortia, M. Pule, T. Marafioti, M. Gore, J. Larkin, S. Turajlic, C. Swanton, K. S. Peggs, S. A. Quezada, Fc effector function contributes to the activity of human anti-CTLA-4 antibodies. *Cancer Cell* **33**, 649–663.e4 (2018).
81. A. P. F. do Rosario, T. Lamb, P. Spence, R. Stephens, A. Lang, A. Roers, W. Muller, A. O'Garra, J. Langhorne, IL-27 promotes IL-10 production by effector Th1 CD4+ T cells: A critical mechanism for protection from severe immunopathology during malaria infection. *J. Immunol.* **188**, 1178–1190 (2012).
82. J. Brummelman, E. M. C. Mazza, G. Alvisi, F. S. Colombo, A. Grilli, J. Mikulak, D. Mavilio, M. Alloisio, F. Ferrari, E. Lopci, P. Novellis, G. Veronesi, E. Lugli, High-dimensional single cell analysis identifies stem-like cytotoxic CD8⁺ T cells infiltrating human tumors. *J. Exp. Med.* **215**, 2520–2535 (2018).
83. J. Brummelman, C. Haftmann, N. G. Nunez, G. Alvisi, E. M. C. Mazza, B. Becher, E. Lugli, Development, application and computational analysis of high-dimensional fluorescent antibody panels for single-cell flow cytometry. *Nat. Protoc.* **14**, 1946–1969 (2019).
84. L. W. Collison, D. A. Vignali, In vitro Treg suppression assays. *Methods Mol. Biol.* **707**, 21–37 (2011).
85. M. I. Love, W. Huber, S. Anders, Moderated estimation of fold change and dispersion for RNA-seq data with DESeq2. *Genome Biol.* **15**, 550 (2014).

Downloaded from https://www.science.org at Cardiff University on December 15, 2024

Erratum for the Research Article “Acquisition of suppressive function by conventional T cells limits antitumor immunity upon T_{reg} depletion” by S. K. Whiteside *et al.*

There are multiple corrections to the Research Article “Acquisition of suppressive function by conventional T cells limits antitumor immunity upon T_{reg} depletion” by S. K. Whiteside *et al.* There were typographic errors in the text labels of specific genes within heatmaps in Fig. 1C, wherein the gene *Ifngr1* was mistakenly labeled as “*Ifng*”; Fig. 3E, wherein the gene *Cxcl2* was mistakenly labeled as “*Cxcl12*”; Fig. 4A, wherein the gene *Cxcl3* was mistakenly labeled as “*Cxcl13*”; and fig. S1, wherein the gene *Sema4f* was mistakenly labeled as “*Semaf4a*.“ The graphical alignment of text labels corresponding to genes within heatmaps have also been corrected in Fig. 1C and fig. S1, which mistakenly represented labels to prior versions of the heatmaps. This did not affect the graphically represented membership of any gene within annotated clusters in fig. S1. In the corrected Fig. 1C, *Ccl5* is shown in cluster A rather than cluster B, *Pdcld1* is shown in cluster B rather than cluster D, and *Runx2* is shown in cluster B rather than cluster E. The following statement in the Results section has been corrected so as not to refer to *Runx2* as a member of cluster E: “cluster E comprised a limited set of T_{reg} cell–specific transcripts that were not expressed at high relative levels in CD4 $^{+}$ or CD8 $^{+}$ T_{conv} cells even upon T_{reg} depletion, including *Foxp3*, *Lrrc32*, *Ikzf2*, and *Ctla4*.“ Collectively, these typographic and graphical corrections to gene labels of the heatmaps do not change the underlying bioinformatics analyses or the raw data in the associated data files. The overall conclusions of the article remain unchanged.